FISSION YIELD STUDIES AND CLOSED SHELL EFFECTS IN ATOMIC NUCLEI

FISSION YIELD STUDIES AND CLOSED SHELL EFFECTS IN ATOMIC NUCLEI

by

ROBERT KENNETH WANLESS M.Sc.

A Thesis

Submitted to the Faculty of Arts and Science

in Partial Fulfilment of the Requirements

for the Degree

Doctor of Philosophy

McMaster University

October 1953

DOCTOR OF PHILOSOPHY (1953)
(Physics)

McMASTER UNIVERSITY
Hamilton, Ontario

TITLE: Fission Yield Studies and Closed Shell Effects in Atomic Nuclei.

AUTHOR: Robert Kenneth Wanless, B.Sc. (McMaster University)
M.Sc. (McMaster University)

SUPERVISOR: Dr. H. G. Thode

NUMBER OF PAGES: 62

SCOPE AND CONTENTS:

The relative fission yields of the isotopes of krypton and xenon have been determined mass spectrometrically. Abnormal fission yields, resulting in fine structure in the mass fission yield curve, have been found in both mass ranges. A shift of the fine structure to lower masses has been observed in going from U^{235} + n fission to U^{238} + n fission. From this shift in fine structure it has been possible to determine the proportions of U^{235} and U^{238} neutron fission that have occurred in the sample. Evidence is presented to show that the observed fine structure and the shift in this fine structure is the result of a combination of two effects involving the extra stability of closed neutron shells of 50 and 82 neutrons which fall in the Kr and Xe ranges respectively.

The capture of thermal neutrons by Xe^{135}, which modifies the fission yields in the 135 and 136 mass chains, has been studied so that the observed fission yields at these masses may be suitably corrected.

Finally, the branching ratio between the isomeric states of

Kr^{85} and the half-life of the long-lived isomer have been re-determined and found to be 0.29 and 10.27 $\pm$ 0.18 yrs. respectively.

ACKNOWLEDGEMENTS

The author wishes to express his sincere appreciation for the encouragement and inspiration of Dr. H. G. Thode under whose direction this work has been carried out. He also wishes to thank Mr. W. H. Fleming for many helpful discussions and for assistance with the analysis of an uranium sample.

Financial assistance from the following organizations is gratefully acknowledged:

National Research Council, Studentship, 1951-52

Research Council of Ontario, Scholarship, 1952-53 (resigned)

National Cancer Institute of Canada, Fellowship, 1952-53

The work has been made possible through the financial assistance of the National Research Council of Canada. The author wishes to thank the Atomic Energy of Canada Limited both for financial aid and for arranging the irradiation of uranium samples at Chalk River and at United States Atomic Energy Commission establishments.

TABLE OF CONTENTS

LIST OF FIGURES

LIST OF TABLES

INTRODUCTION

Nuclear reactions resulting in the fission of heavy nuclei are among the most interesting, and widely studied, nuclear processes known today. The fission act may be a spontaneous reaction (1,2) or an induced reaction brought about by the bombardment of the nucleus with particles (3) or electromagnetic radiation (4). The object of this particular investigation has been to compare abnormal fission yields which occur in the krypton and xenon mass ranges (in the neighbourhood of the 50 and 82 neutron shells) for U^{235} and U^{238} neutron induced fission and to determine the proportions of U^{235} and U^{238} fission that occur in nuclear reactors under various irradiating conditions. In addition the extent of capture of thermal neutrons by Xe^{135} has been studied by measuring the increase of the Xe^{136} fission yield caused by this reaction. The half-life of the long-lived isomer of Kr^{85} and the branching ratio between the isomeric states of Kr^{85} have been precisely determined.

The neutron induced fission of the uranium isotope of atomic weight 235 may be described as follows:

$$ {}_{92}U^{235} + {}_{0}n^{1} \longrightarrow {}_{92}U^{236} \longrightarrow {}_{Z_1}A_1 + {}_{Z_2}A_2 + \nu\, n + Q \qquad \ldots(1) $$

$$ Z_1 + Z_2 = 92 $$

$$ A_1 + A_2 = 236 - \nu $$

A thermal neutron is captured by U^{235} to form a compound nucleus with atomic weight 236. This nucleus is in a highly excited state and

breaks into two lighter fragments with atomic weights A_1 and A_2 and atomic numbers Z_1 and Z_2 respectively. In addition ν neutrons are released (2.5 neutrons per fission act in U^{235} (5)) as well as approximately 200 Mev. of energy, Q.

Radiochemical determinations (6) of the yields of the mass fragments resulting from fission have shown that, in general, $A_1 \neq A_2$. Rather it has been found that the nucleus divides in an asymmetric fashion and the most abundant yields occur in the neighbourhood of 94 and 140 mass units. When the logarithms of the fission yields, determined radiochemically, (6) are plotted against mass number two distinct maxima result as shown in Fig. 1. It will be noted that symmetric fission, i.e. $A_1=A_2 \doteq 117$, is about 600 times less probable than the asymmetric division to masses in the neighbourhood of 94 and 140 mass units.

The smooth curve illustrated in Fig. 1 is determined from the cumulative yield of the various masses and does not represent the distribution at the instant of fission. Since the neutron to proton ratio is higher than the stable ratio in this region of the periodic table, the primary fission products are unstable and undergo successive β^- disintegrations which change the atomic number by one unit but do not alter the mass number. It has been shown that the fission fragments achieve stability after approximately three β^- disintegrations (7) and the release of about 11 Mev. of energy. Tables I and II list several of the fission chains resulting from successive β^- disintegrations and ending in the stable isotopes of Kr, Rb, Sr, Xe, Cs and Ba.

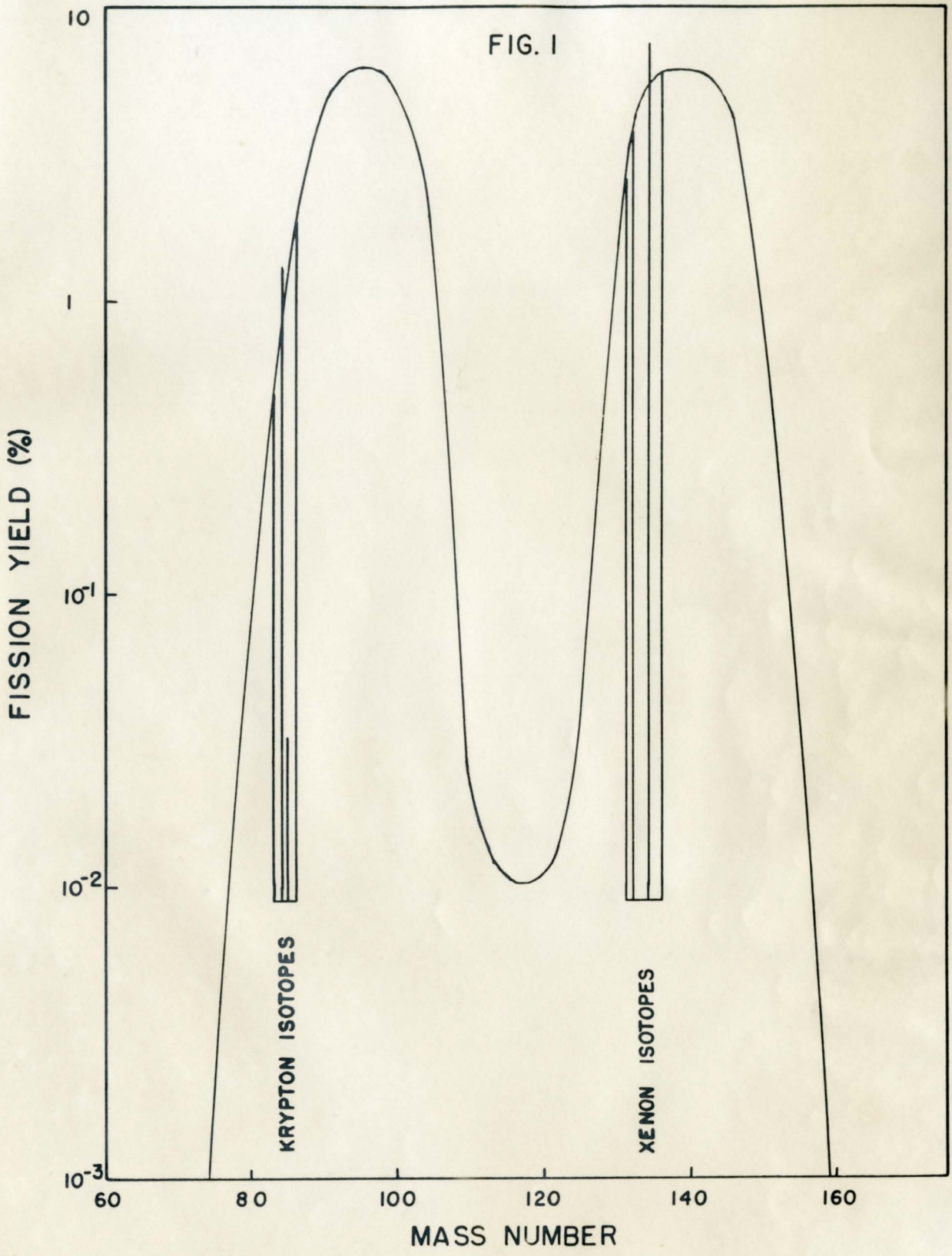

MASS YIELD CURVE FOR THERMAL NEUTRON FISSION OF U^{235}

TABLE I

FISSION PRODUCT CHAINS IN THE LOW MASS RANGE

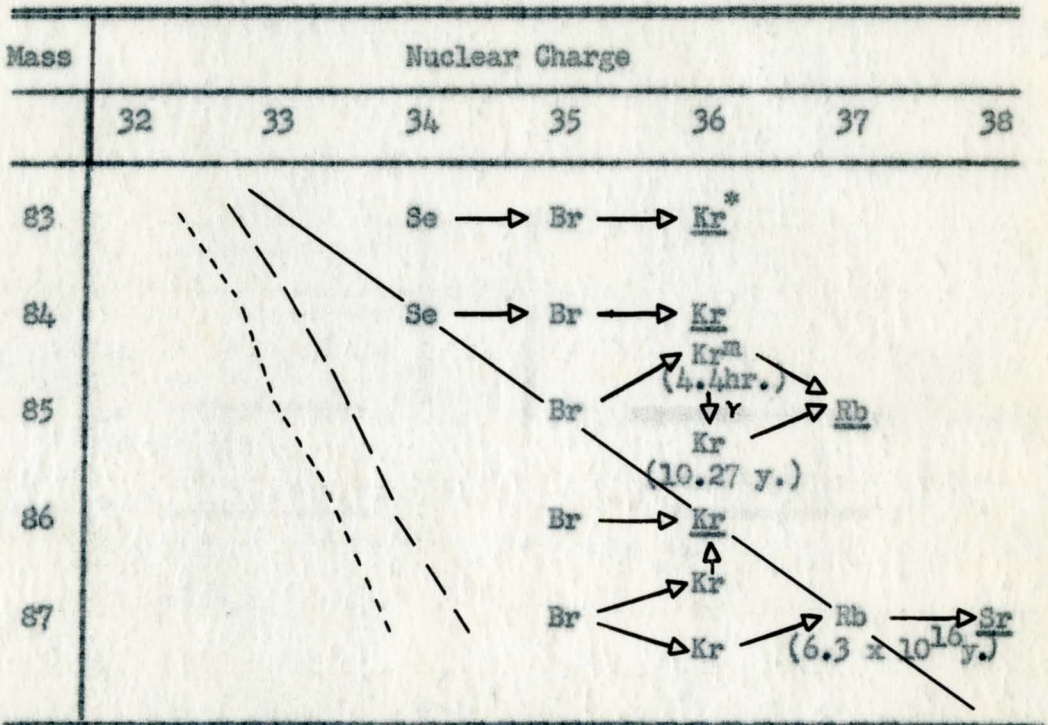

*Stable end products are underlined.

Vertical arrows represent the emission or absorption of a neutron

—— 50 neutron nuclides

— — Z_p U^{235} + n. Calculated from postulate of equal charge displacement.

----- Z_p U^{238} + n. " " " " " " " (12)

TABLE II

FISSION PRODUCT CHAINS IN THE HIGH MASS RANGE

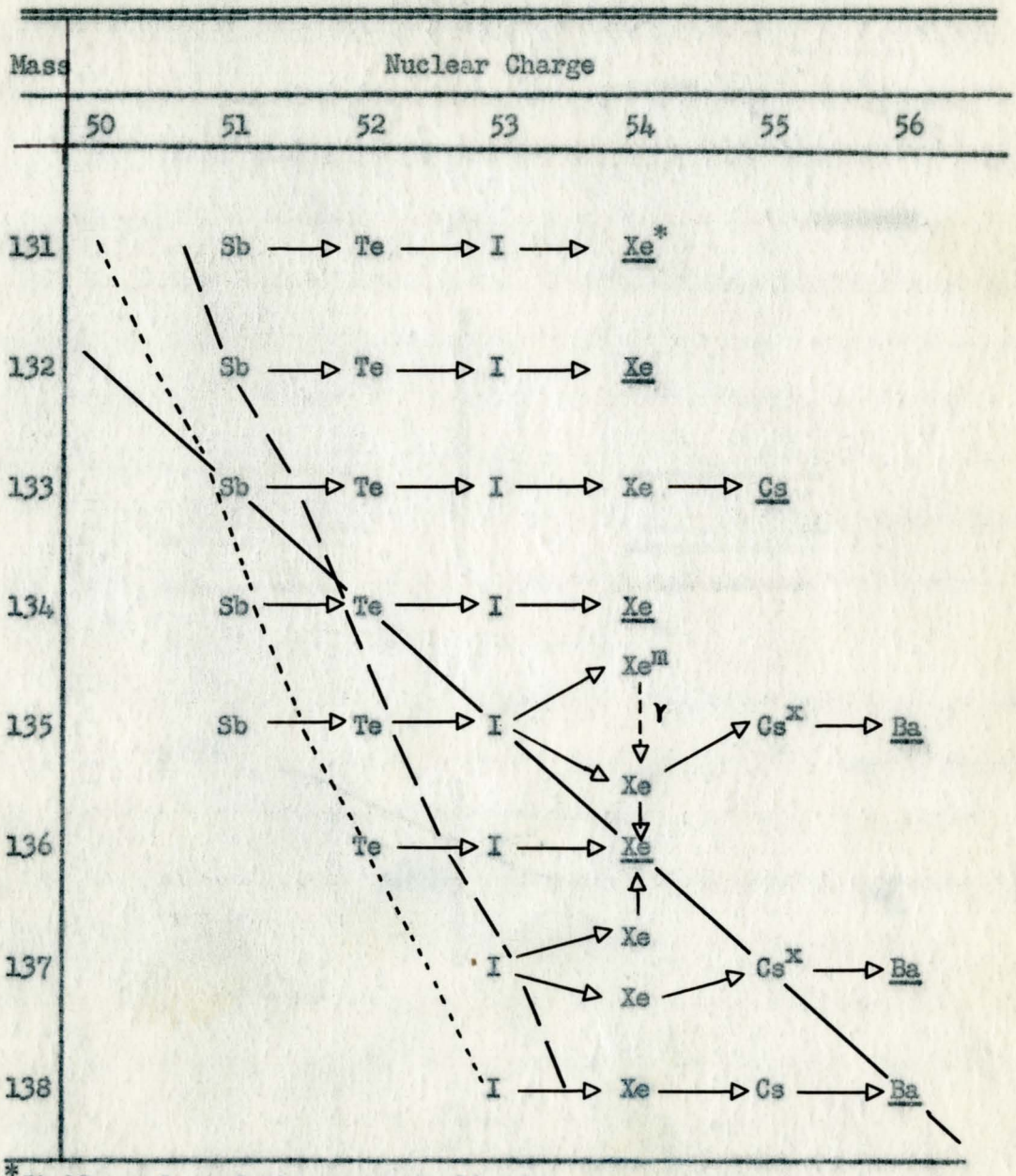

*Stable end products are underlined.

Vertical arrows represent the emission or absorption of a neutron.

—— 82 neutron nuclides

— — Z_p U^{235} + n. Calculated from postulate of equal charge displacement (12).

------- Z_p U^{238} + n " " " " " " "

xCs^{135} and Cs^{137} have half-lives of 2.1 x 10^6 yrs. and 33 yrs. respectively and their yields may be measured mass spectrometrically with the stable end products.

Thode and Graham (8) used a mass spectrometer to determine the relative yields of the fission product chains ending in the stable rare gases Kr and Xe. By this method relative yields of the stable isotopes that grow from the active fission products or are formed as primary fission products may be determined with an accuracy of ± 1% or better. This accuracy is much better than can be obtained using standard radiochemical techniques. When a suitable point of normalization is chosen these mass spectrometer yields may be combined with the radiochemical yield data to precisely determine the shape of the fission yield curve in the mass regions from mass 83 to 86 and from mass 131 to 136. Thode and co-workers (9, 10) have also studied the adjacent fission chains ending in the stable or long-lived isotopes of Rb, Sr, and Cs (see Tables I and II).

Macnamara, Collins and Thode (11) have shown that some of the Xe yields determined mass spectrometrically do not fall on the smooth fission yield curve drawn from the radiochemical data. Specifically they have found that in the fission of U^{235} with thermal neutrons the yields of the 133 and 134 mass chains are high by 26% and 35% respectively. It has been postulated by Glendenin (12) that this fine structure of the mass yield curve may be due to the extra stability of nuclides with 82 neutrons which fall in the Xe mass range. Mayer (13) has recently summarized the experimental facts which indicate that nuclides with shells of 50, 82 and 126 neutrons are particularly stable configurations and Harvey (14) has shown that the binding energy of the 51st, 83rd., and 127th neutron is about 2 Mev lower than the binding energy of the 50th, 82nd, and 126th neutron. Glendenin suggested

that nuclides formed as primary fission products with one more neutron than a closed shell will evaporate this extra neutron rather than undergo β^- disintegrations as is usually the case. The Glendenin mechanism, however, requires that gains to one fission chain must be balanced by losses to adjacent chains. The predicted decreases at masses 135 and 136 corresponding to the high yields at masses 133 and 134 have not been observed experimentally (9). It has been suggested (15, 9) therefore, that in addition to the Glendenin mechanism, nuclides with 82 neutrons are favoured in the primary fission process and that the observed fine structure is a combination of these two effects. One would expect the latter effect to be a function of the distance of the nuclide from the Bohr-Wheeler stability curve and to increase as we go from mass 131 to 136 while the Glendenin effect, which depends on the instability of the 83rd neutron should decrease as the Bohr-Wheeler stability curve is approached. Empirical curves to represent the variation of these effects have been established (15, 9) and fair agreement with experimental results has been obtained.

Glendenin and co-workers (16) have also reported fine structure in the 98-100 mass range where the Mo isotopes have high fission yields. By folding the fission yield curve for the heavy mass peak over the light mass peak in such a way that the masses of complimentary fission products sum to 233.5 they have shown that the fine structure in the two mass ranges (i.e. 98-100 and 131-136) coincides. These results confirm the suggestion of Wiles et. al. (15, 9) that some fine structure is a result of a structural preference in the initial fission act since it is difficult to explain the high Mo yields from the point of view of closed

neutron shells in that range. There is, however the possible exception of extra stability of the 40 proton shell in this mass range and Duckworth and Preston (17) have found a break in the packing fraction curve which they attribute partly to the stability of this configuration.

Considerable information may be obtained about the fission process by studying the variations in the complete fission yield curve resulting from the fission of different nuclei when bombarded by high energy particles as well as thermal neutrons. The fission yield curves for U^{238} and Pu^{239} have been established (6) and are plotted with the U^{235} fission yield curve in Fig. 2. Several striking differences in the shape of the curves are observed. Generally the U^{235} thermal neutron fission yield curve is more symmetrical about its mid-point at mass 117. The shift to the heavier masses required to account for the greater mass in U^{238} and Pu^{239} is made up almost entirely of a shift of the lighter mass peak. The peak to trough ratio varies considerably, indicating that symmetric fission yields have increased by a factor of four for U^{238} fission.

Spence (18) has determined the variation of U^{235} fission yields with neutron energy and finds that symmetric fission increases by a factor of 100 when the energy of the neutrons increases from thermal energies to 14 Mev. Turkevich and co-workers (19, 20) have established the yield curves for the fission of Th^{232} with 2.6 Mev. pile neutrons and fast neutrons from the Li + D reaction and report that symmetric fission yields increase by a factor of ten for the higher energy neutrons. Schmitt and Sugarman (21) have produced fission in natural

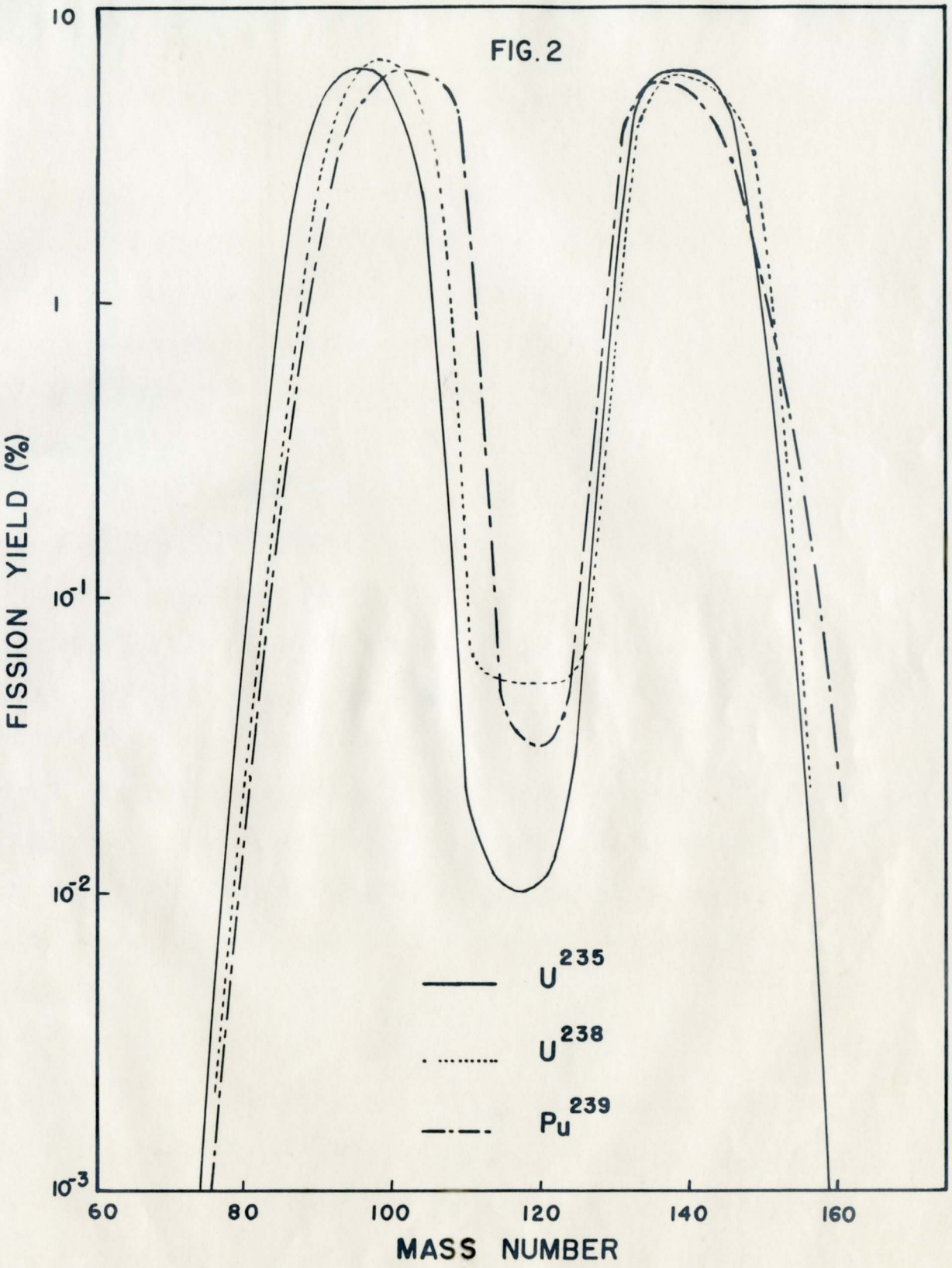

MASS YIELD CURVES FOR NEUTRON FISSION OF U^{235}, U^{238} AND Pu^{239}

uranium by means of x-rays of energies ranging from 22 to 100 Mev and find that symmetric yields increase by a factor of 100 for 48 Mev x-rays as compared to the yield observed for U^{235} thermal neutron fission. Turkevich et al. (20) have shown that the peak to trough ratio increases over a range of 300 when high energy fission yields are compared with the yields for thermal neutron induced fission. Meitner (22) has reported completely symmetric fission for deuteron induced fission of Bi^{199}.

It is apparent that a more symmetric type of fission occurs when higher energy particles or electromagnetic radiations bombard the fissioning nucleus. While the complete fission yield curve cannot be established from the rare gas data the extent of yield variations in the Kr and Xe mass ranges resulting from the above mentioned effects may be precisely determined.

Assuming the postulate of equal charge displacement (12) (i.e. equal fission chain lengths for the two fission fragments) it is possible to calculate the most probable charge, Z_p, for a given mass, to be expected for the primary fission products from the following formula:

$$Z_p = Z_A - 0.5\,(Z_A + Z_{(233.5 - A)} - 92) \qquad \ldots(2)$$

Where Z_A represents the most stable charge (non-integral) for a given mass A (according to Bohr-Wheeler (23)). Z_A and $Z_{(233.5 - A)}$ are the most stable charges for the given chain and its complimentary fission chain respectively. The equation may be modified for fissioning nuclei other than U^{235} by substituting the appropriate values in place of 233.5 and 92.

The Z_p values for U^{235} and U^{238} have been calculated and lines have been drawn through these points in Table II. It will be noted that the Z_p - 235 line crosses the line joining nuclides with 82 neutrons in the region of masses 133 and 134 which have been observed to have abnormally high fission yields in U^{235} fission. Since the Z_p - 238 line intersects the 82 neutron line at lower masses it may be expected that the fine structure will shift toward the lower mass range (132 and 133) in U^{238} fission.

Since it has been observed in this laboratory that the high fission yield at mass 134 is not constant but varies with irradiation conditions or pile position or both, it was felt that this variation may be due to shift of the fine structure resulting from different proportions of U^{235} and U^{238} fission and experiments were planned to investigate this effect further. Uranium metal and uranium oxide samples have been irradiated under conditions such that the resulting fission will be that of U^{235}, U^{238} or mixtures of these. Once the Xe fission yields are known for the two nuclei it should be possible to determine the proportion of U^{235} and U^{238} fission that has taken place during irradiation.

Although it is felt that fine structure should also occur in the Kr range in the neighbourhood of the 50 neutron shell its existence had not been definitely established. The Kr isotopes fall farther down the side of the light mass peak and their yields change rapidly due to the steepness of the mass yield curve in this region. As a result of their position farther down the side of the peak the fission yields are lower than the Xe yields by a factor of five and mass

spectrometric determinations are usually less precise. The lines joining the Z_p values and the 50 neutron nuclides have been drawn in Table I. It will be noted that the Z_p lines do not cross the 50 neutron line within the Kr range under study and hence fine structure would not be expected to occur here. However, these Z_p values were calculated on the assumption that the fission chain lengths are the same in both mass regions and consequently the Z_p lines fall at lower Z values. Since the fission chains appear to be shorter here the Z_p line may be shifted toward higher Z values and cross the 50 neutron line in the Kr isotope range. It is possible, then, that some fine structure may occur here and an extensive investigation of this region was carried out, the results of which are reported in this thesis.

In order to determine the fission yields it is necessary to consider certain reactions which result in fission chain branching. The variation in the 135 and 136 mass chain due to the reaction -

$$Xe^{135} + n \longrightarrow Xe^{136} \qquad \ldots (3)$$

is important since Xe^{135} has a high neutron capture cross-section in the thermal neutron range. The extent of capture of neutrons by this isotope is of interest for two reasons. First, in order to determine the fission yields, the 136 mass chain ending in stable Xe^{136} (Table II) must be decreased while the fission yield of the 135 mass chain ending in 33 yr. Cs^{135} must be increased by an amount dependent on the extent of the above reaction. Secondly, since the capture cross-section of Xe^{135} for thermal neutrons is so large its presence must be considered in pile design and operation.

The vertical arrows (Table II) from Xe^{135} and Xe^{137} represent the capture of a thermal neutron by Xe^{135} and the delayed release of a neutron by Xe^{137}. Both of these reactions tend to increase the fission yield of Xe^{136}. The emission of a neutron by Xe^{137} is thought to be constant (0.2% of fission) but the percentage increase of Xe^{136}, resulting from the capture of a neutron by Xe^{135} will be a function of the thermal neutron flux and the length of time the sample has been irradiated in the pile.

Calculations of the increase to be expected in the 136 mass chain resulting from reaction 3 have been carried out. The ratio of the amount of Xe^{136} produced by neutron capture in Xe^{135} to the amount resulting from the decay of I^{136} is given by -

$$\frac{Xe^{136}\uparrow_{Xe^{135}}}{Xe^{136}\uparrow_{I^{136}}} = \frac{\int_{t=0}^{t=T} (\text{No. atoms } Xe^{135} \text{ present at any time t}).\ F.\sigma_c\, Xe^{135}\, dT}{Y_{I^{136}} \cdot f \cdot T} \qquad \ldots(4)$$

F = thermal neutron flux $n/cm^2/hr.$

$\sigma_c\, Xe^{135}$ = thermal neutron capture cross section for Xe^{135}.

$Y_{I^{136}}$ = fission yield of I^{136}.

f = total number of fissions per hour.

T = irradiation time in hours.

The number of atoms of Xe^{135} present at any time, t, may be calculated as follows:

$$\frac{dN_{Xe135}}{dt} = \lambda_{I135}N_{I135} - \lambda_{Xe135}N_{Xe135} - \sigma_{c_{Xe135}}N_{Xe135} \cdot F$$

or $$\frac{dN_1}{dt} = \lambda_2 N_2 - KN_1 \qquad \ldots (5)$$

where $$K = \lambda_{Xe135} + \sigma_{c_{Xe135}} \cdot F \qquad \ldots (6)$$

The number of atoms of I^{135}

$$\frac{dN_{I135}}{dt} = Y_{I135} \cdot f - \lambda_{I135}N_{I135}$$

or $$\frac{dN_2}{dt} = Y_2 \cdot f - \lambda_2 N_2 \qquad \ldots (7)$$

Integrating and assuming that $N_2 = 0$ at time $t = 0$ we get

$$N_2 = \frac{Y_2 \cdot f}{\lambda_2}\left[1 - e^{-\lambda_2 t}\right] \qquad \ldots (8)$$

Substituting in equation 5, integrating and employing limits

$N_1 = 0$ at time $t = 0$ we get

$$N_1 = Y_2 \cdot f \cdot \left[\frac{1}{K} - \frac{e^{-\lambda_2 t}}{(K-\lambda_2)} - \frac{e^{-Kt}}{K} + \frac{e^{-Kt}}{(K-\lambda_2)}\right] \qquad \ldots (9)$$

Substituting equation 9 in equation 4, integrating and employing limits

$t = 0$ to $t = T$ we get

$$F\sigma_{c_{Xe135}}\int_{t=0}^{t=T} N_1 \cdot dT = F \cdot \sigma_{c_{Xe135}} \cdot Y_2 \cdot f \cdot \left[\frac{T}{K} + \frac{e^{-\lambda_2 T}}{\lambda_2(K-\lambda_2)} + \frac{e^{-KT}}{K^2} - \frac{e^{-KT}}{K(K-\lambda_2)} - \frac{1}{\lambda_2(K-\lambda_2)}\right.$$

$$\left. - \frac{1}{K^2} + \frac{1}{K(K-\lambda_2)}\right] \qquad \ldots (10)$$

$$= F\sigma_{c_{Xe135}} \cdot Y_2 \cdot f \cdot Q \qquad \ldots (11)$$

Substituting equation 11 in equation 4 we obtain finally

$$\frac{Xe^{136} \uparrow}{Xe^{135} \uparrow} = \frac{Y_I 135 \cdot f \cdot Q \cdot F \cdot \overline{\sigma}_{cXe^{135}}}{Y_I 136 \cdot f \cdot T} \qquad \ldots (12)$$

Figure 3 is a plot of equation 12 showing the percentage increase of Xe^{136} for various flux values from 10^{11} to 10^{14} thermal neutrons/cm.^{2}/sec. and for irradiation times sufficiently long to produce 10^{17} and 10^{18} fissions in the uranium sample. In addition the curve for a constant irradiation time of seventy hours has been plotted.

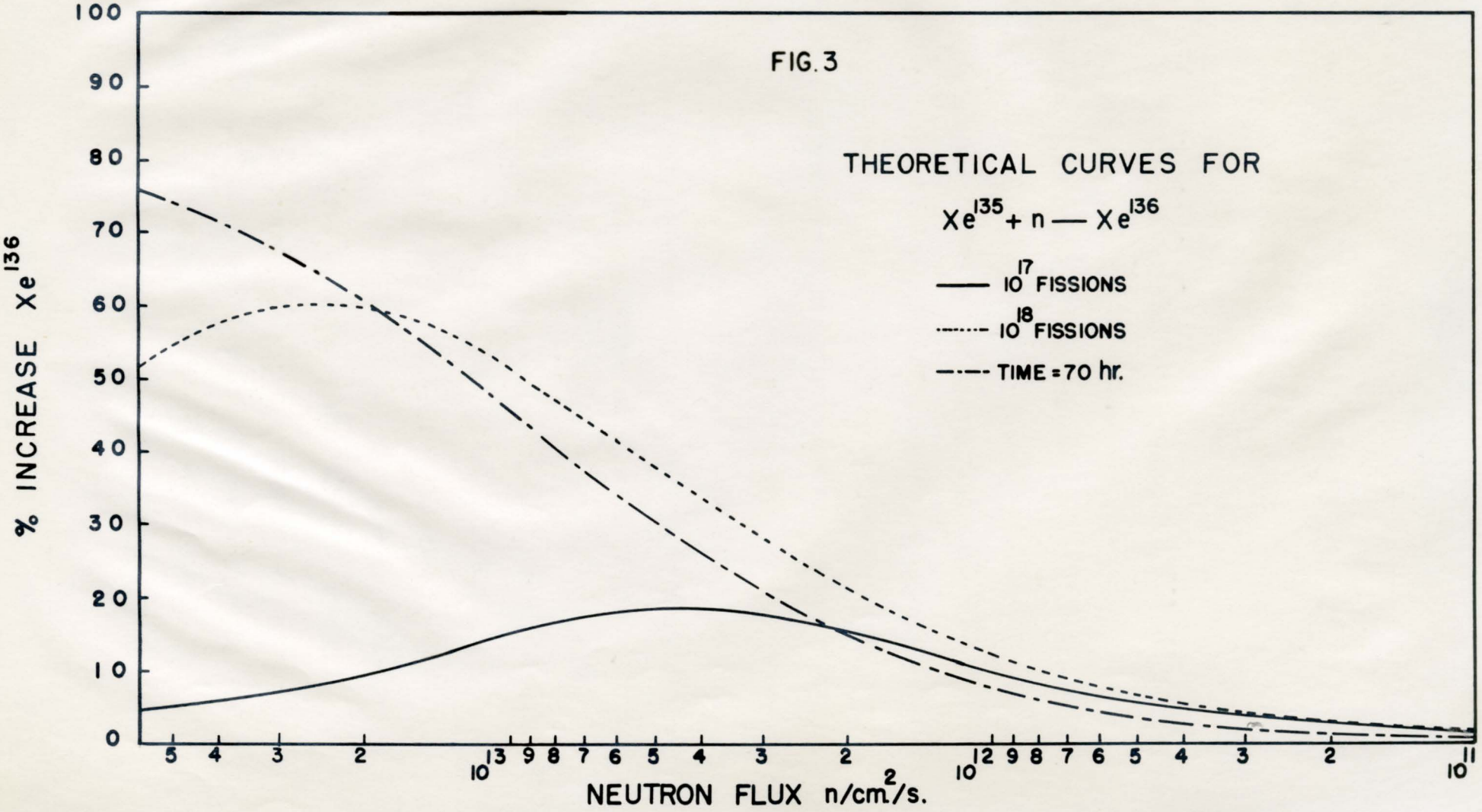
FIG. 3
THEORETICAL CURVES FOR
$Xe^{135} + n \rightarrow Xe^{136}$
10^{17} FISSIONS
10^{18} FISSIONS
TIME = 70 hr.
% INCREASE Xe^{136}
NEUTRON FLUX $n/cm^2/s.$
100
90
80
70
60
50
40
30
20
10
0
5 4 3 2 10^{13} 9 8 7 6 5 4 3 2 10^{12} 9 8 7 6 5 4 3 2 10^{11}

EXPERIMENTAL

I SAMPLE PREPARATION

Uranium samples weighing from 10 to 50 gms. were irradiated, at as nearly a constant flux as possible, for periods long enough to produce approximately 10^{17} fissions. Previous work (8) in this laboratory had shown that sufficient fission product xenon and krypton gas (10^{-3} cc. at N.T.P.) for mass spectrometric analysis was produced when this number of fissions had occurred. In most cases the irradiated materials were allowed to "cool" for sufficient time after removal from the pile, for all the precursors to decay to the stable rare gas isotopes.

The rare gases were extracted from the uranium using the method described by Arrol, Chackett and Epstein (24). The extraction and purification apparatus is illustrated in Fig. IV. Concentrated cupric potassium chloride in flask F1, was thoroughly flushed with dry hydrogen from reservoir H, to eliminate the air dissolved in the solution. The hydrogen which had been previously dried and purified by passage through an activated charcoal trap cooled to liquid nitrogen temperature was passed through the solution in F1 by manipulation of stopcocks T1, T2, T3, and T4. The uranium disc was placed in a platinum basket which was suspended from a curved glass rod whose movement could be controlled from outside the vacuum system through a greased standard taper joint in the wall of flask F_2. After the sample had been placed in F_2 the vessel was evacuated through T_5. Hydrogen was now allowed to flow into F_1 through T_3 to force the cupric potassium chloride solution into F_2 via

FIG. 4

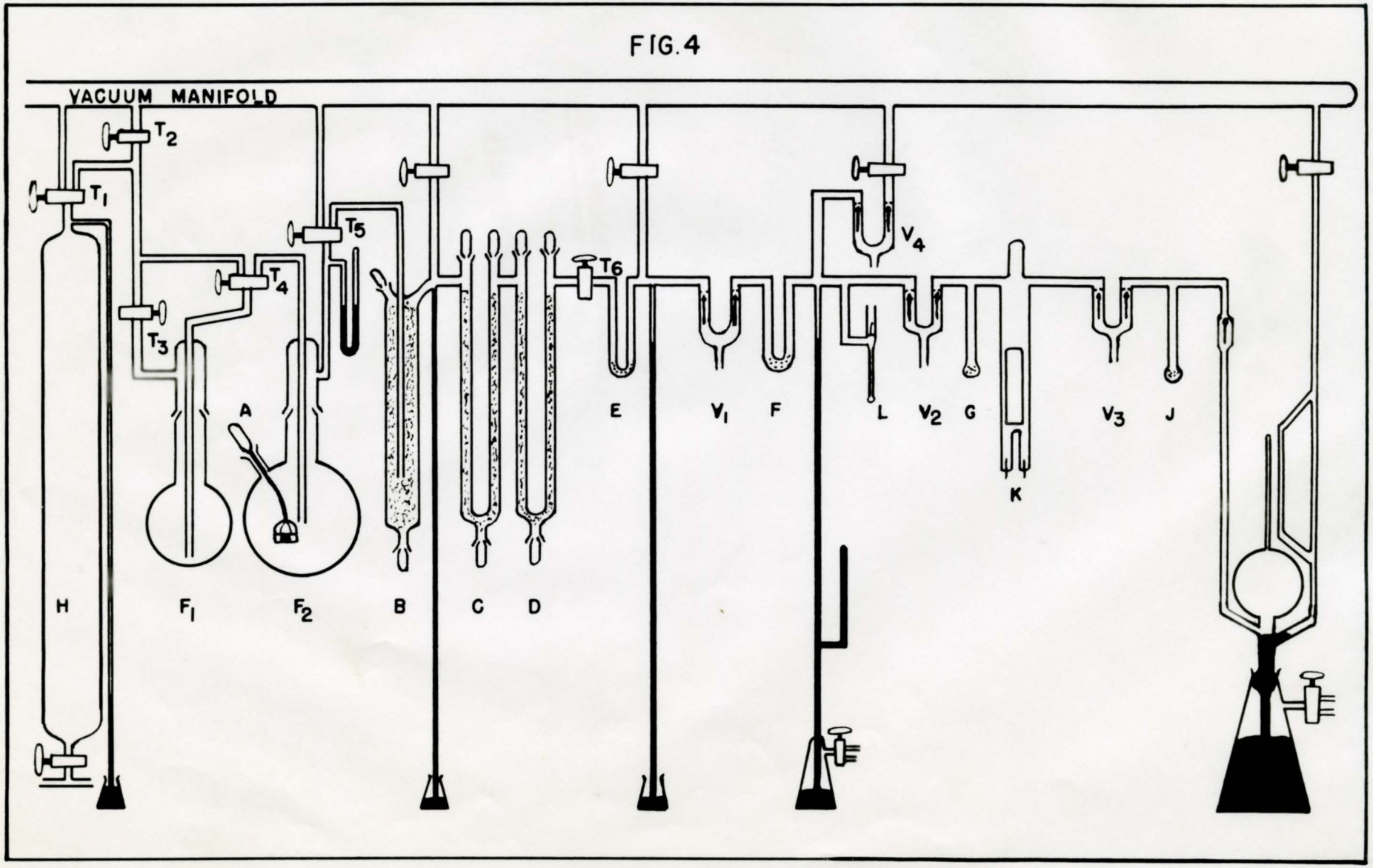

RARE GAS EXTRACTION & PURIFICATION APPARATUS

stopcock T_4. The rate of dissolution of the metal was controlled by raising or lowering the platinum basket in F_2. The liberated gases were allowed to flow through T_5 into the drying trap B, containing solid potassium hydroxide pellets, through two U tubes C and D, containing anhydrous magnesium perchlorate and finally through T_6 into charcoal trap E, which was cooled in liquid air. From this point the gases were manipulated using standard high vacuum technique. Mercury ventils V_1, V_2, V_3 and V_4 replace all stopcocks to avoid possible absorption of the rare gases in the stopcock grease.

By warming F and cooling charcoal tube G in liquid air the gas mixture was moved to the section of the apparatus containing the calcium furnace K. After exposure to Ca vapours at 450° to 500° C for about 20 minutes the residual gas volume was measured in the calibrated McLeod gauge. The Ca purification procedure was repeated until the volume of the gas remained constant. The purified gas was then condensed in charcoal tube L, at liquid air temperature and the tube was sealed off from the vacuum line.

Tube L was designed to facilitate the introduction of the gas sample to the mass spectrometer for analysis. A small iron slug was sealed in the tube above the glass break-off and the upper portion evacuated on the mass spectrometer sample line. The iron slug was then raised by means of small permanent magnets and allowed to strike the glass break-off. The gas was then transferred to the mass spectrometer sample line where it was condensed in a similar charcoal tube until analysis could be carried out.

Usually a three to four mm^3 gas sample, at N.T.P., made up

of argon, krypton and xenon, was collected, the argon being present due to the fact that the uranium metal was originally processed in an argon atmosphere.

II MASS SPECTROMETRY

All gas samples were analysed on a 180 degree direction focusing mass spectrometer (8). Magnetic scanning was employed throughout to focus ions of 1500 volts energy. An Applied Physics Corporation Model 30 vibrating reed amplifier was used to amplify the ion current which was recorded on a Leeds and Northrup Speedomax strip chart recorder. Typical isotope patterns for fission product krypton and xenon are shown in Figs. 5 and 6 respectively. At least ten double sets of peaks were recorded and averaged for each analysis.

Care was taken to insure that there were no residuals in the mass spectrometer before the samples were admitted and each sample was checked for impurities in the neighbourhood of the krypton and xenon mass ranges. To remove any condensable impurities that may be present in the samples a liquid air trap was used between the sample input line and the mass spectrometer.

As an indication of the reproducibility of results over long periods of time reference is here made to Tables XIII and XIV of this thesis where the analysis of the same gas sample, carried out after six years, is compared with the original result. It will be noted that the percentage difference in the two results was never greater than $\pm$ 1%.

FIG. 5

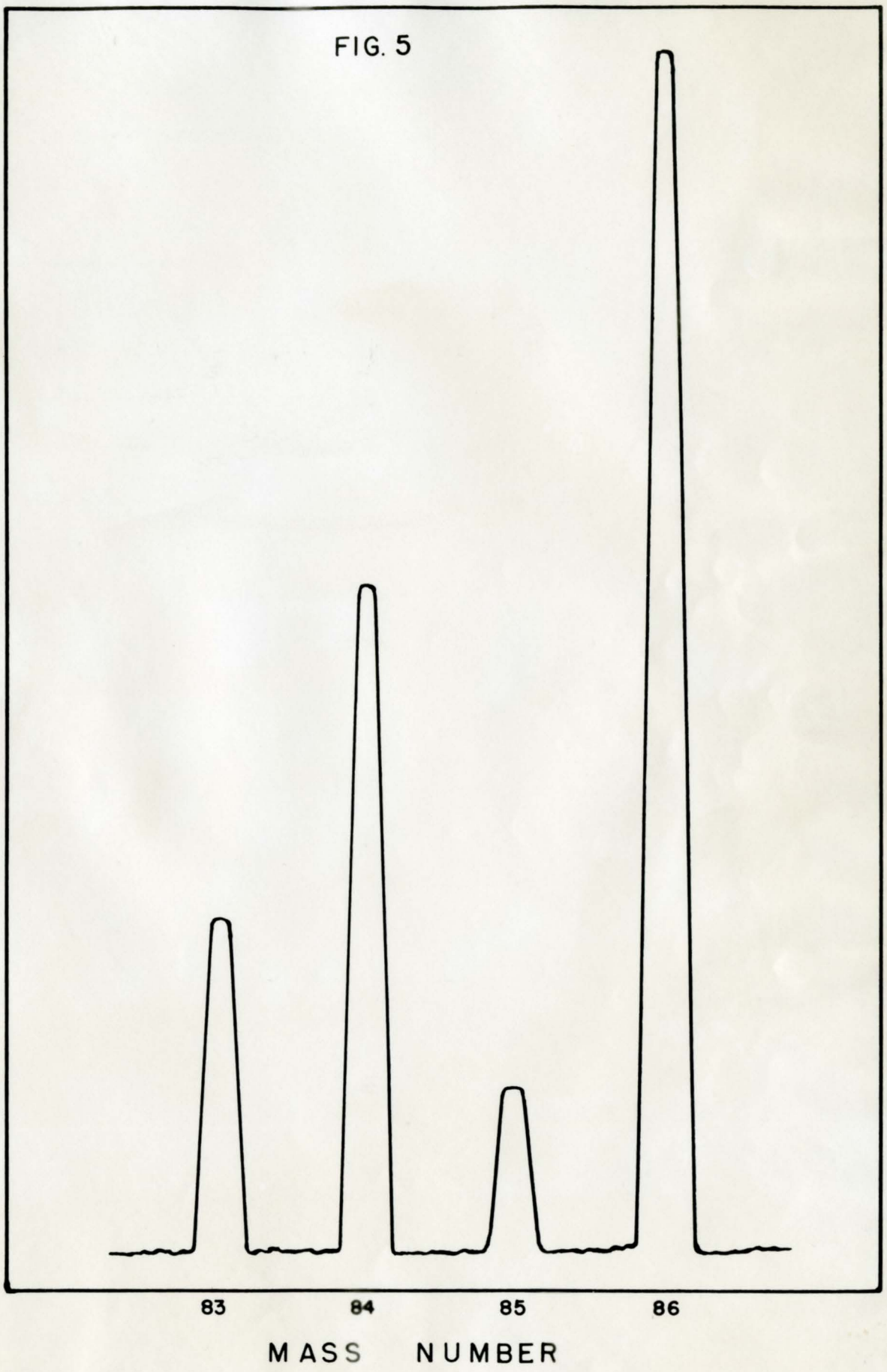

FIG. 6

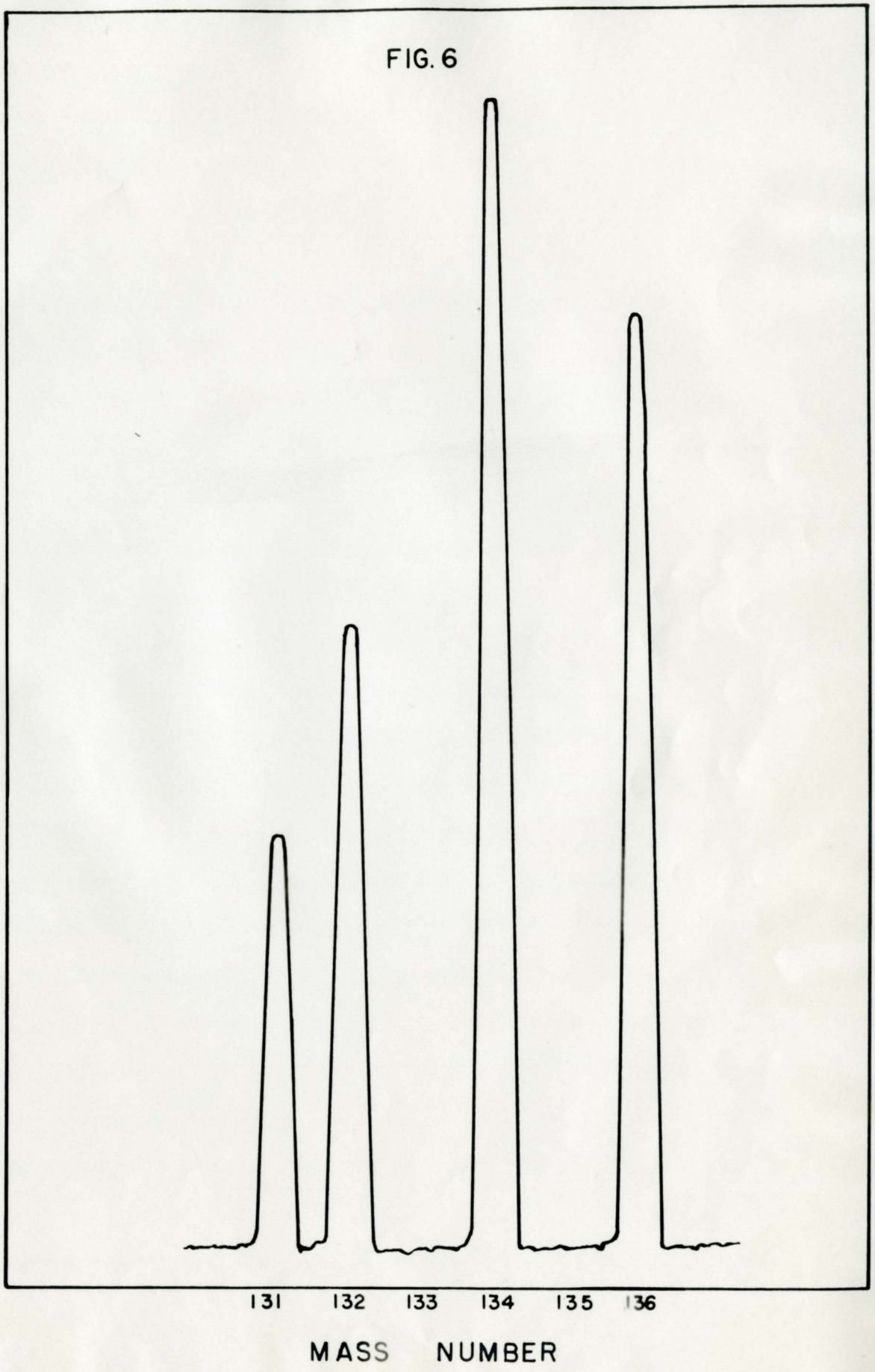

III RESULTS

(i) The Resonance Capture of Thermal Neutrons by Xe^{135}

The extent of capture of thermal neutrons by Xe^{135} has been determined, mass spectrometrically, by following the variations in the Xe^{136} fission yield as a function of the neutron flux. Samples for investigation were irradiated at various flux positions of the Chalk River N.R.X. and Oak Ridge Reactors (Table III). One disc, No. 12, was irradiated in a cadmium sheath. Since cadmium has a high absorption cross section in the thermal neutron range and up to one electron volt (25), the energy range in which the resonance capture of Xe^{135} occurs, the percentage increase in the fission yield of Xe^{136} due to reaction 3 should be negligible in this sample. The results obtained for the cadmium sheathed sample are, therefore, used as a base level from which the extent of reaction 2 may be calculated.

In some cases the uranium discs were dissolved before all the precursors of Xe^{131} and Xe^{132} (see Table II) had decayed completely and corrections to the 131 and 132 fission yields for the amount of precursor still present at the time of dissolution have been carried out.

Table IV gives the mass spectrometer abundance data for the isotopes of fission product xenon for the samples investigated. The xenon fission yields at masses 131, 132, 134 and 136 are normalized at a value of 3.28% for the 131 mass chain (9). The Xe^{136}/Xe^{131} ratio is plotted as a function of the neutron flux in Fig. 7 where the curve has been drawn through the experimental points using the method of least squares.

Originally the change in the Xe^{136}/Xe^{134} ratio was used to

TABLE III

URANIUM IRRADIATION DATA

Sample No.	Nuclear reactor	Time in reactor	Neutron flux * neutrons/cm.^{2}/sec.
1	N.R.X. Chalk River	11 hrs.	5×10^{13}
2	" "	20 hrs.	6×10^{12}
3	" "	35.5 hrs.	3.6×10^{12}
4	" "	35 days	3×10^{12}
5	" "	34.5 hrs.	2.6×10^{12}
6	" "	12 hrs.	2.6×10^{12}
7	" "	57 hrs.	2.1×10^{12}
8	" "	68.5 hrs.	1.8×10^{12}
9	" "	70 days	7.5×10^{11}
10(a)(b)	Oak Ridge	16 days	6×10^{11}
11	N.R.X. Chalk River	68 days	1×10^{11}
12[x]	" "	11.5 days	1.5×10^{13}

*Flux values for N.R.X. Reactor were estimated from data contained in Chalk River Report No. C.R.E. 414 - "Some Data on Pile Irradiation" by I. L. Wilson (26).

[x]Sample No. 12 was irradiated in a cadmium sheath. See text.

TABLE IV

MASS SPECTROMETER ABUNDANCE DATA FOR THE ISOTOPES OF FISSION PRODUCT XENON*

SAMPLE NO.	% FISSION YIELD			
	MASS UNIT			
	131	132	134	136
1	3.28	4.89	8.95	8.70
2	3.28	4.91	8.84	7.93
3	3.28	4.92	8.95	7.86
4	3.28	4.99	9.11	8.11
5	3.28	4.92	9.02	8.17
6	3.28	4.92	8.88	7.72
7	3.28	4.91	8.95	7.74
8	3.28	4.94	9.03	8.04
9	3.28	4.93	8.99	7.81
10 (a)	3.28	4.92	8.93	7.64
10 (b)	3.28	4.91	8.80	7.52
11	3.28	4.91	8.98	7.26
12	3.28	4.97	8.71	7.08

*Xenon isotope abundances at masses 131, 132, 134 and 136 have been normalized at 3.28% for mass 131 determined radiochemically for I131.

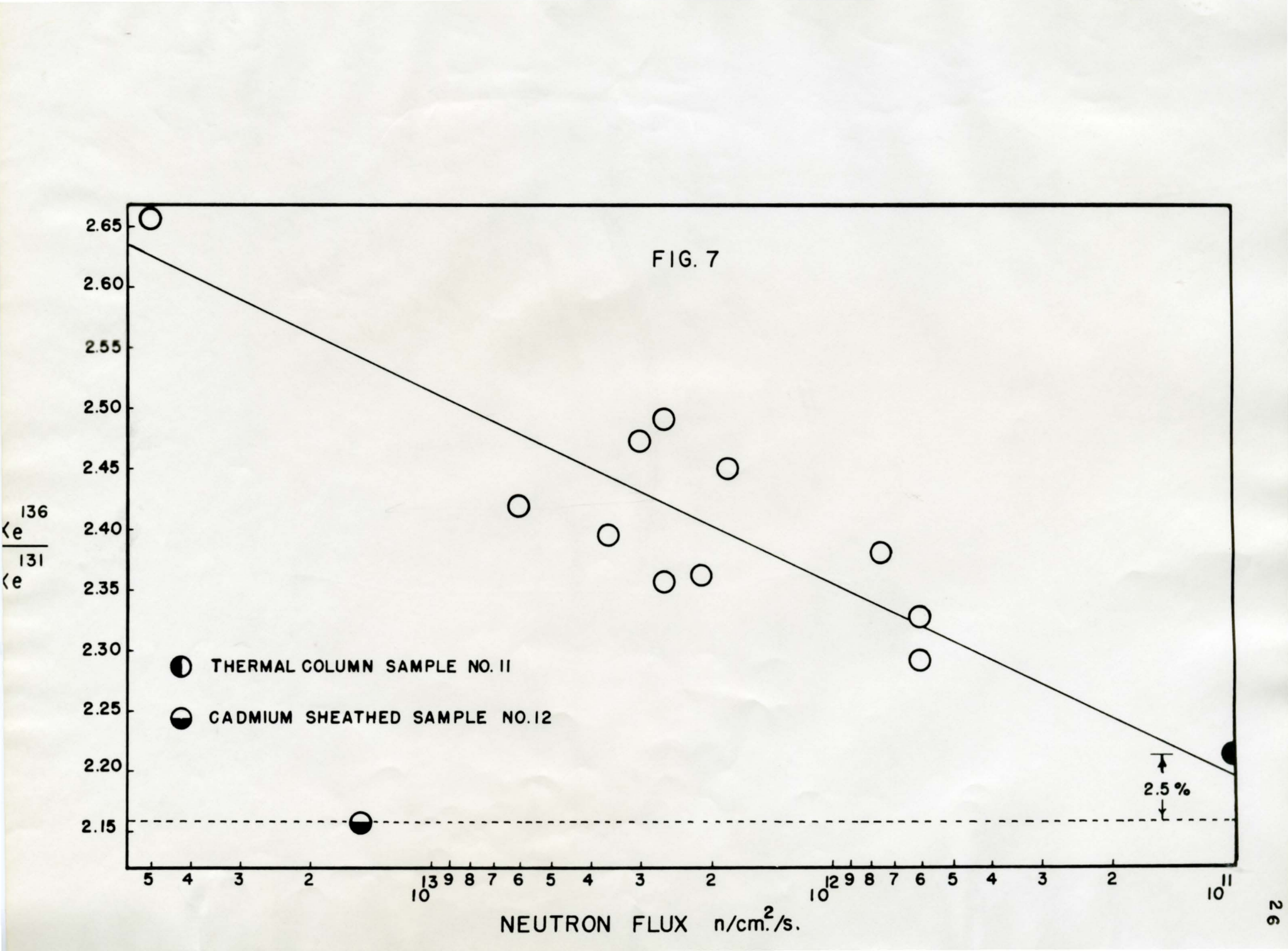
FIG. 7
2.65
2.60
2.55
2.50
2.45
2.40
2.35
2.30
2.25
2.20
2.15
136 Xe / 131 Xe
THERMAL COLUMN SAMPLE NO. 11
CADMIUM SHEATHED SAMPLE NO. 12
2.5 %
5 4 3 2 10^13 9 8 7 6 5 4 3 2 10^12 9 8 7 6 5 4 3 2 10^11
NEUTRON FLUX n/cm.²/s.

establish the Xe^{135} burning correction to the Cs^{135} and Xe^{136} fission yields but considerable variation in this ratio was found for a group of samples irradiated in the N.R.X. reactor during the months of April and September 1951. These variations indicated that not only was the 136 fission yield varying, due to neutron capture in Xe^{135}, but that the other xenon isotope yields were also functions of the irradiating conditions. Recently uranium discs (sample No. 11, Table III) were irradiated in the thermal column of the N.R.X. reactor at a neutron flux of 10^{11} $n/cm^2/sec$. The xenon fission yields determined for this sample and the cadmium sheathed sample (No. 12) are plotted in Fig. 8 where the smooth curve has been arbitrarily drawn through the thermal column yields at masses 131, 132 and 136. It is noted that the yields for the two samples differ at masses 132, 134 and 136 by 1.2%, 3.1%, and 2.5% respectively. The 2.5% difference at mass 136 should be largely due to the burning of Xe^{135} in the thermal column sample. On the other hand the variations in the 132 and 134 mass yields cannot be explained by neutron capture processes. The high percentage of fast neutrons (50% of the thermal neutron flux (26)) available for fission of the cadmium sheathed sample suggests the possibility of some U^{238} + n fission superimposed on the U^{235} + n fission.

In view of the fact that the 132 and 134 yields for the cadmium sheathed sample vary with respect to the thermal column yields the Xe^{136}/Xe^{134} and Xe^{136}/Xe^{132} ratios determined for this sample could not be used to establish the Xe^{135} burning correction. Therefore, the Xe^{136}/Xe^{131} ratio which is considered the most reliable was used for this purpose.

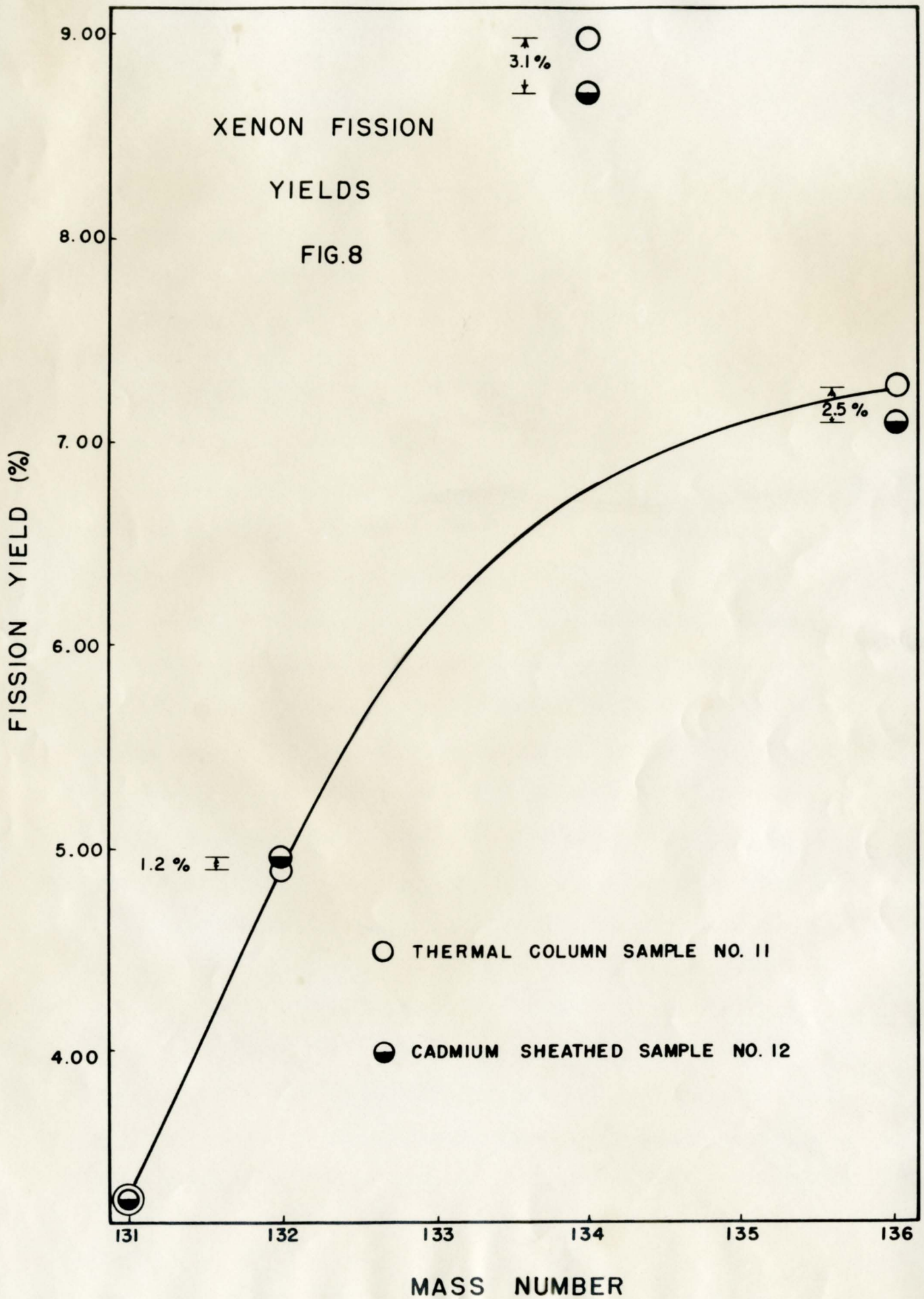
XENON FISSION
YIELDS
FIG.8
9.00
8.00
7.00
6.00
5.00
4.00
FISSION YIELD (%)
3.1 %
2.5 %
1.2 %
THERMAL COLUMN SAMPLE NO. 11
CADMIUM SHEATHED SAMPLE NO. 12
131
132
133
134
135
136
MASS NUMBER

Xe^{135} burning corrections determined from the Xe^{136}/Xe^{131} ratio (Fig. 7) are in good agreement with theoretical values taken from the curves of Fig. 3, in the medium flux range. In establishing the theoretical curves a capture cross section of 2.8×10^6 barns for Xe^{135} was used and the fission yields of I^{135} and I^{136} were assumed to be equal.

(ii) Fine Structure In The Fission Yield Curve For U^{235} and U^{238} Neutron Fission

(a) Xenon

Mass spectrometer fission yield studies have shown that the Xe^{134} fission yield is abnormally high for U^{235} + n fission (11). Since this fine structure in the mass fission yield curve has been attributed to the stable neutron configuration of 82 neutrons it would be interesting to determine whether the fine structure remains unchanged or if it shifts to other masses for the fission of different nuclei. A shift in the fine structure would explain the results of the preceding section. In order to investigate this effect further the following irradiations were carried out. Normal uranium discs were irradiated in the thermal column of the N.R.X. reactor at a neutron flux of 1×10^{11} thermal neutrons/cm^2/sec.; UO_3 powder depleted about 30 to 50 times in U^{235} was irradiated for six months in the Los Alamos Fast Reactor at a neutron flux of about 10^{12} neutrons/cm^2/sec. with an average energy of 0.5 Mev.; finally, normal uranium samples were irradiated in the Los Alamos Reactor for periods ranging from two to five months also at a flux of approximately 10^{12} neutrons/cm^2/sec. The detailed irradiation data are given in Table V and the mass spectrometer

TABLE V

URANIUM IRRADIATION DATA

Sample No.	Nuclear reactor	Irradiation particulars	Time in reactor	Neutron flux* neutrons/$cm.^2$/sec.
11	N.R.X. Chalk River	Normal U thermal column	68 days	1×10^{11}
12	" "	Normal U Cd sheathed	11.5 days	1.5×10^{13}
13	Los Alamos Fast Reactor	Normal U	65 days	10^{12}
14	" "	Normal U	166 days	10^{12}
15	" "	UO_3 Depleted in U^{235}	192 days	10^{12}

*Flux values for Chalk River irradiations are for the thermal neutron flux. Los Alamos irradiations were carried out in a fast neutron flux with an average energy of 0.5 Mev.

TABLE VI

MASS SPECTROMETER ABUNDANCE DATA FOR ISOTOPES OF FISSION PRODUCT XENON

SAMPLE NO.	% FISSION YIELD			
	MASS UNIT			
	131	132	134	136
11	3.28	4.91	8.98	7.08 x
12	3.28	4.97	8.71	7.08
13 14	3.28	5.20	8.17	7.20
15	3.28 3.77*	4.73 5.43*	6.57 7.55*	5.85 6.72*

x Mass 136 yield has been corrected for thermal neutron capture (see Fig. 7).

* Yields adjusted at mass 136 to indicate the same percentage fine structure shift for the Los Alamos normal uranium sample at masses 132 and 134. See text.

fission yield data are given in Table VI. The thermal column results are the average of three determinations while the UO_3 and normal uranium samples irradiated at Los Alamos were done in duplicate. In all cases the xenon fission yields agreed within the standard deviation of the individual determinations.

The samples are listed (Tables V and VI) in order of increasing amounts of U^{238} fission expected. For example, sample No. 11, irradiated in the thermal column should show little U^{238} + n fission whereas sample No. 15, depleted in U^{235} and irradiated in the Los Alamos Fast Reactor should show little U^{235} + n fission (less than 1%).

The xenon fission yields for samples No. 11 and No. 15 given in Table VI are plotted in Fig. 9, normalized at 3.28% for Xe^{131}. Although the normalization point employed is arbitrary, it is apparent that the relative yields have changed. The 134 fission yield has decreased while the 132 yield has increased for U^{238} + n fission as compared to U^{235} + n fission, indicating a shift in the fine structure to the lower mass range.

Since the mass yield curves for the two fissioning nuclei do not cross in the region of mass 131 (see Fig. II), some other point of normalization must be found in order to compare the fission yields. In Fig. 10 the fission yield data for samples 11, 12, 13 & 14, and 15 (Table VI) have been plotted in the following manner; the thermal column results have been normalized at 3.28% for Xe^{131} as have the results for the Los Alamos normal uranium and cadmium sheathed irradiations. The normalization point for the depleted uranium results (No. 15) has been adjusted (see Table VI) so that the Los Alamos normal uranium yields indicate the same percentage fine structure shift at masses 132 and 134 measured from the smooth curve arbitrarily drawn through the thermal column data at masses 131, 132 and 136. For example,

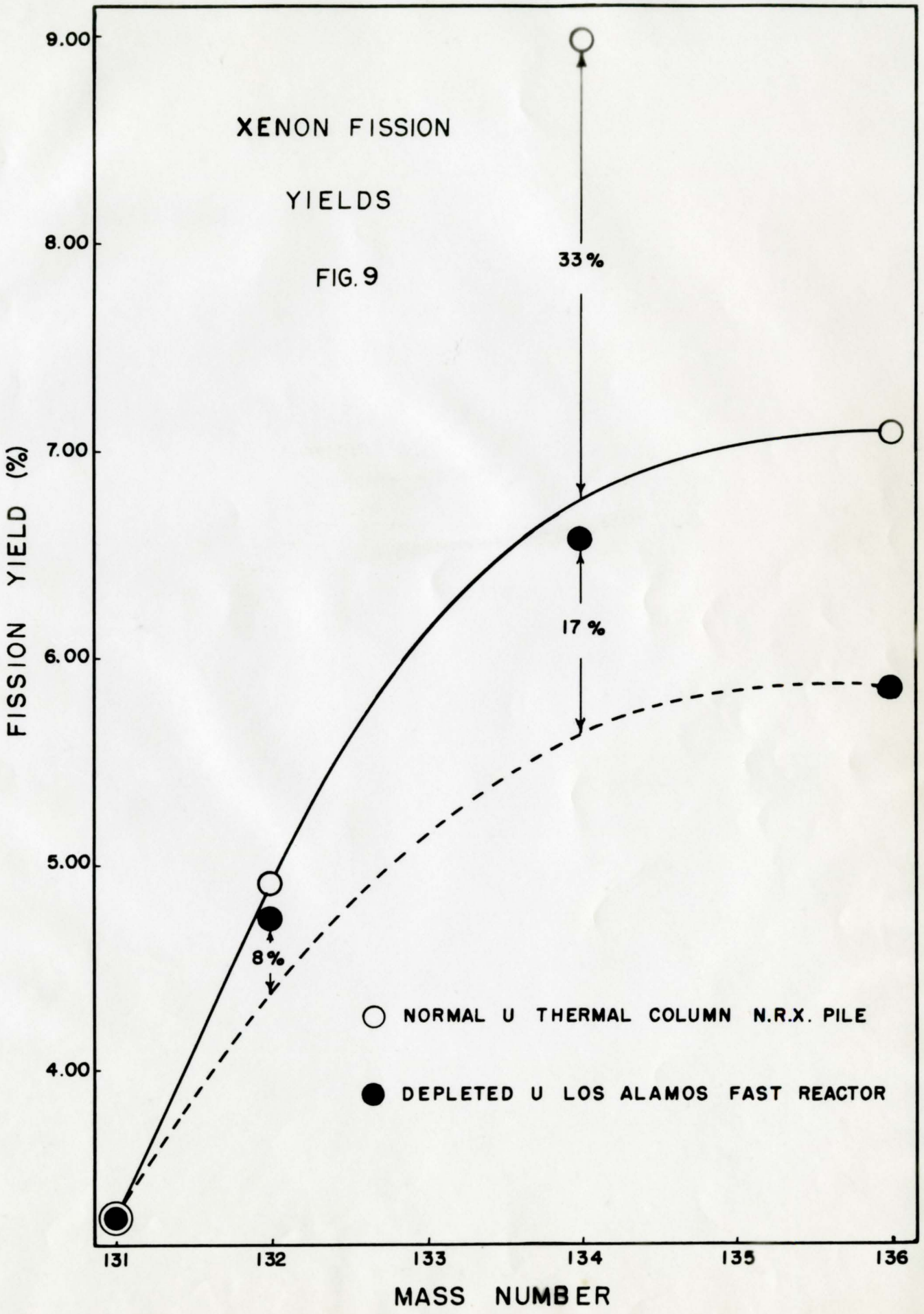
XENON FISSION
YIELDS
FIG. 9
9.00
8.00
7.00
6.00
5.00
4.00
FISSION YIELD (%)
33%
17%
8%
NORMAL U THERMAL COLUMN N.R.X. PILE
DEPLETED U LOS ALAMOS FAST REACTOR
131
132
133
134
135
136
MASS NUMBER

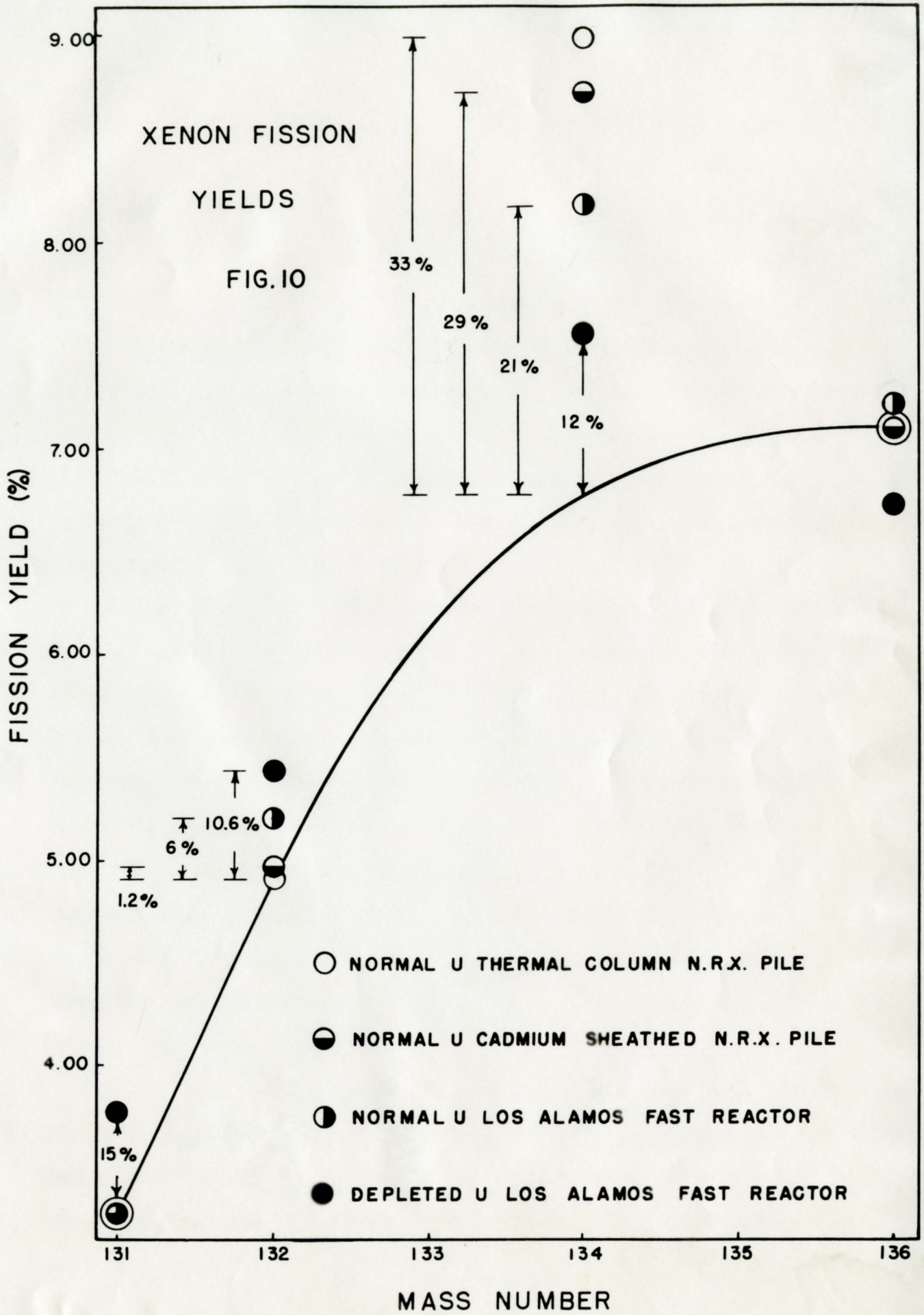
XENON FISSION
YIELDS
FIG. 10
FISSION YIELD (%)
9.00
8.00
7.00
6.00
5.00
4.00
33 %
29 %
21 %
12 %
10.6%
6 %
1.2%
15%
NORMAL U THERMAL COLUMN N.R.X. PILE
NORMAL U CADMIUM SHEATHED N.R.X. PILE
NORMAL U LOS ALAMOS FAST REACTOR
DEPLETED U LOS ALAMOS FAST REACTOR
131
132
133
134
135
136
MASS NUMBER

the fine structure shift at mass 134 in going from U^{235} + n fission (thermal column sample No. 11) to U^{238} + n fission (UO_3 sample No. 15) amounts to 33%-12% = 21%. The shift in fine structure between the thermal column and Los Alamos normal uranium samples (No. 13 & 14) is 33% - 21% = 12%. Therefore the percentage shift in fine structure for the normal uranium irradiated at Los Alamos amounts to 57%. Similarly, at mass 132 the percentage of the total fine structure shift for the Los Alamos normal uranium sample is 6 ÷ 10.6 or 57%. Assuming that the fine structure shift is linear these results indicate that approximately 60% of the fissions occurring in the normal uranium sample were due to U^{238} + n fission while only 40% were due to U^{235} + n fission. Rough calculations from Los Alamos pile data are in agreement with this.

Considering only the UO_3 depleted uranium sample it would appear that the fine structure for U^{238} + n fission decreases at masses 136 and 134 and increases at masses 132 and 131 as compared to the fine structure observed for U^{235} + n fission. The Los Alamos normal uranium results are in agreement with this at masses 132 and 134 but do not agree at masses 131 and 136, the discrepancy amounting to 8% and 5% respectively. A 5% correction for burning of Xe^{135} would bring the 136 mass yield into agreement but it hardly seems probable that reaction 3 could have proceeded to this extent in the Los Alamos reactor where the average neutron energy is 0.5 Mev.

The fine structure shift for the cadmium sheathed sample (Fig. 10) indicates approximately 11% and 19% U^{238} + n fission when calculated from the yield values at masses 132 and 134 respectively. This is rather good agreement in view of the fact that normalization

had to be carried out at mass 131 in spite of the fact that the 131 fission yield has been found to increase due to the shift of fine structure in U^{238} + n fission. It may well be that the fission yield curves for the two uranium nuclei should be tilted with respect to one another in this mass range but it is not possible, from the data available, to determine the amount of tilt that may be required. Fission yields for adjacent mass chains for both U^{235} and U^{238} fission would permit a more accurate location of the smooth curves from which the fine structure could be measured. In order to overcome the normalization problem absolute fission yields must be determined using isotope dilution techniques. Each sample must also be monitored so that the neutron flux at which the irradiation was carried out may be determined. This would involve a tremendous effort but may be essential before the complete picture can be obtained.

It has been suggested by Glendenin (12) that the fine structure observed in the mass yield curve results from the emission of the loosely bound 83rd neutrons from the primary fission products after the initial fission act has taken place. The fission yields predicted by this mechanism for U^{235} + n and U^{238} + n fission have been calculated using the methods employed by Glendenin. The predicted percentage variations from the arbitrarily drawn smooth curve (Figs. 9, 10) are given in Table VII, column six. The corresponding experimental fission yields and variations from the smooth curve are given in columns four and five respectively. A decrease in the fine structure at mass 134 and an increase at masses 132 and 131 is predicted in going from U^{235} + n fission to U^{238} + n fission, as found experimentally. However, this

TABLE VII

COMPARISON OF EXPERIMENTAL AND PREDICTED XENON FISSION YIELDS

Fissioning nuclide	Mass chain	Smooth Curve yields* %	M.S. yields %	Departure from smooth curve %	Departure predicted by Glendenin mechanism %
U^{235}	131	3.28	3.28	-	+ 2.7
	132	4.91	4.91	-	+14.5
	133	6.13	-	-	+20
	134	6.77	8.98	+ 33	+17.7
	135	7.03	-	-	- 1.1
	136	7.08	7.08	-	-17.2
U^{238}	131	3.28	3.77	+ 15	+16.8
	132	4.91	5.43	+ 10.6	+25.5
	133	6.13	-	-	+21.9
	134	6.77	7.55	+ 12	- 2.4
	135	7.03	-	-	-19.1
	136	7.08	6.72	-5.4	-16.2

*Smooth curve arbitrarily drawn. (Figs. 9, 10).

mechanism requires that gains in one fission chain must be balanced by losses in adjacent chains and consequently a decrease is predicted at masses 135 and 136. While the results reported here do not permit a check of the 135 mass chain the large predicted decrease at mass 136 has not been observed. It seems, therefore, that the fine structure cannot be wholly due to the Glendenin effect but may be a combination of this effect and some preference for nuclides with 82 neutrons in the primary fission process as suggested by Wiles, et al. (15, 9) and discussed in the introduction.

(b) Krypton

Krypton fission yields have also been determined for those samples irradiated for the study of the extent of capture of thermal neutrons by Xe^{135} (Table III). The mass spectrometer abundance data are given in Table VIII and the Kr^{86}/Kr^{84}, Kr^{86}/Kr^{83}, Kr^{85}/Kr^{83} and Kr^{84}/Kr^{83} ratios are plotted in Figs. 11, 12, 13 and 14 respectively, where the curves have been drawn using the method of least squares. It is apparent that while the 83, 85 and 86 fission yields remain relatively constant (less than 1% variation) with flux, the 84 fission yield varies by 3 to 4%. This variation in Kr^{84} yield again suggested the possibility of fine structure in the mass yield curve in this mass range and the variation of this fine structure with irradiating conditions. Results obtained for the thermal column and Los Alamos irradiated samples (Nos. 11, 13, 14 and 15) bear this out (Table IX). The yields for these samples are plotted in Fig. 15 where the thermal column (No. 11) and Los Alamos normal uranium results (Nos. 13 & 14) have been normalized, arbitrarily, at a value of 0.50% at mass 83. Unfortunately absolute

TABLE VIII

MASS SPECTROMETER ABUNDANCE DATA FOR ISOTOPES OF FISSION PRODUCT KRYPTON

SAMPLE NO.	ATOM %			
	MASS UNIT			
	83	84	85*	86
1	13.89	27.27	7.45	51.40
2	13.99	27.89	7.22	50.90
3	14.12	26.69	7.57	51.63
5	13.88	26.67	7.44	52.02
8	14.16	26.38	7.66	51.80
9	14.17	26.50	7.50	51.83
10 (a)	14.11	26.64	7.61	51.64
10 (b)	14.18	26.72	7.61	51.49
11	14.12	26.25	7.53	52.10
12	14.05	26.76	7.69	51.51

*Kr^{85} yields have been corrected for the decay of the 10.27 yr. isomer.

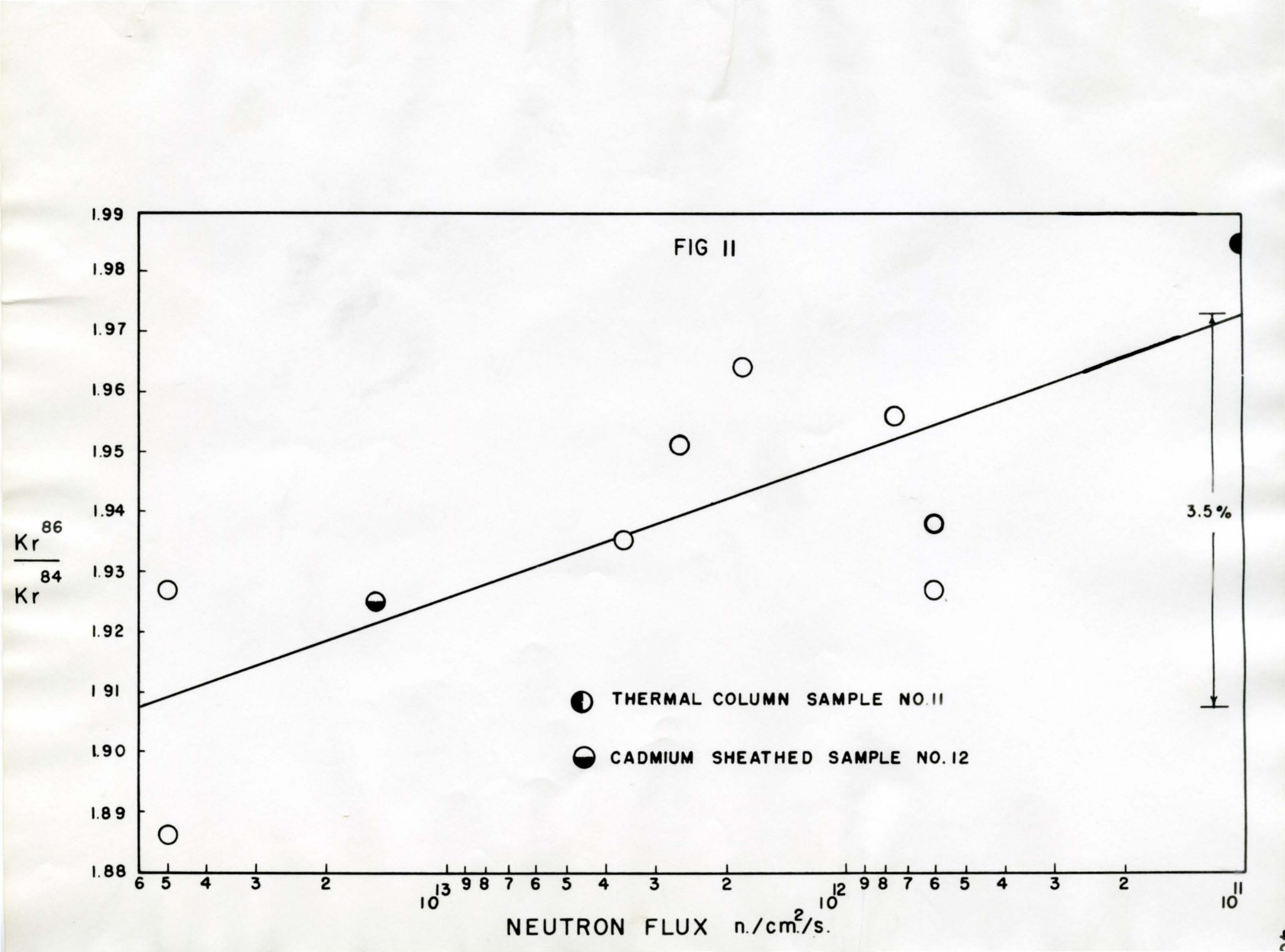
FIG II
1.99
1.98
1.97
1.96
1.95
1.94
1.93
1.92
1 91
1.90
1.89
1.88
Kr 86 / Kr 84
3.5 %
THERMAL COLUMN SAMPLE NO.11
CADMIUM SHEATHED SAMPLE NO. 12
6 5 4 3 2 10^13 9 8 7 6 5 4 3 2 10^12 9 8 7 6 5 4 3 2 10^11
NEUTRON FLUX n./cm.²/s.

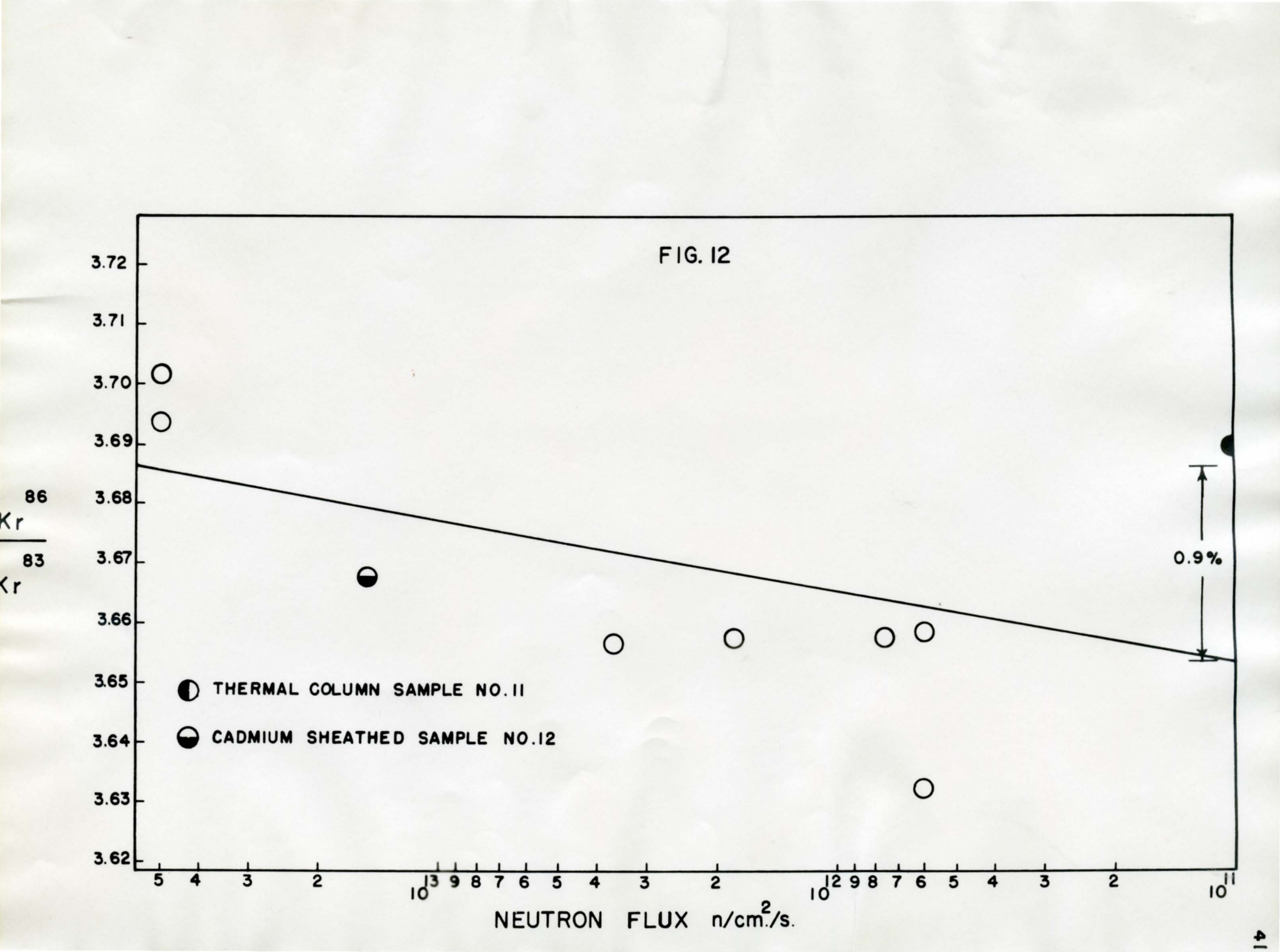
FIG. 12
3.72
3.71
3.70
3.69
3.68
3.67
3.66
3.65
3.64
3.63
3.62
86
Kr
83
Kr
0.9%
THERMAL COLUMN SAMPLE NO. 11
CADMIUM SHEATHED SAMPLE NO. 12
5 4 3 2 10^13 9 8 7 6 5 4 3 2 10^12 9 8 7 6 5 4 3 2 10^11
NEUTRON FLUX n/cm.^2/s.

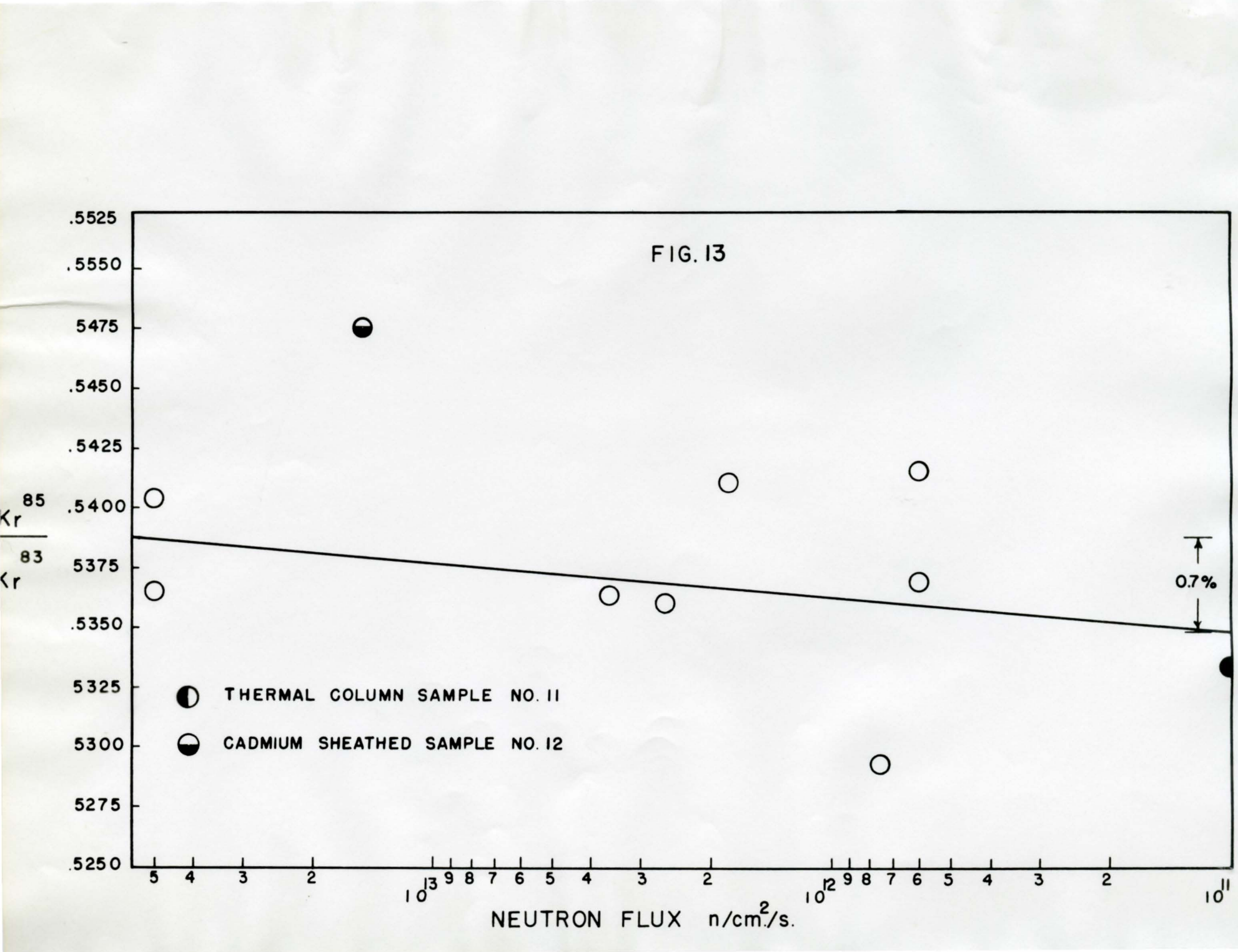
FIG. 13
.5525
.5550
5475
.5450
.5425
.5400
.5375
.5350
5325
5300
5275
.5250
$\frac{Kr^{85}}{Kr^{83}}$
0.7%
THERMAL COLUMN SAMPLE NO. 11
CADMIUM SHEATHED SAMPLE NO. 12
5 4 3 2 10^{13} 9 8 7 6 5 4 3 2 10^{12} 9 8 7 6 5 4 3 2 10^{11}
NEUTRON FLUX n/cm.^{2}/s.

FIG. 14

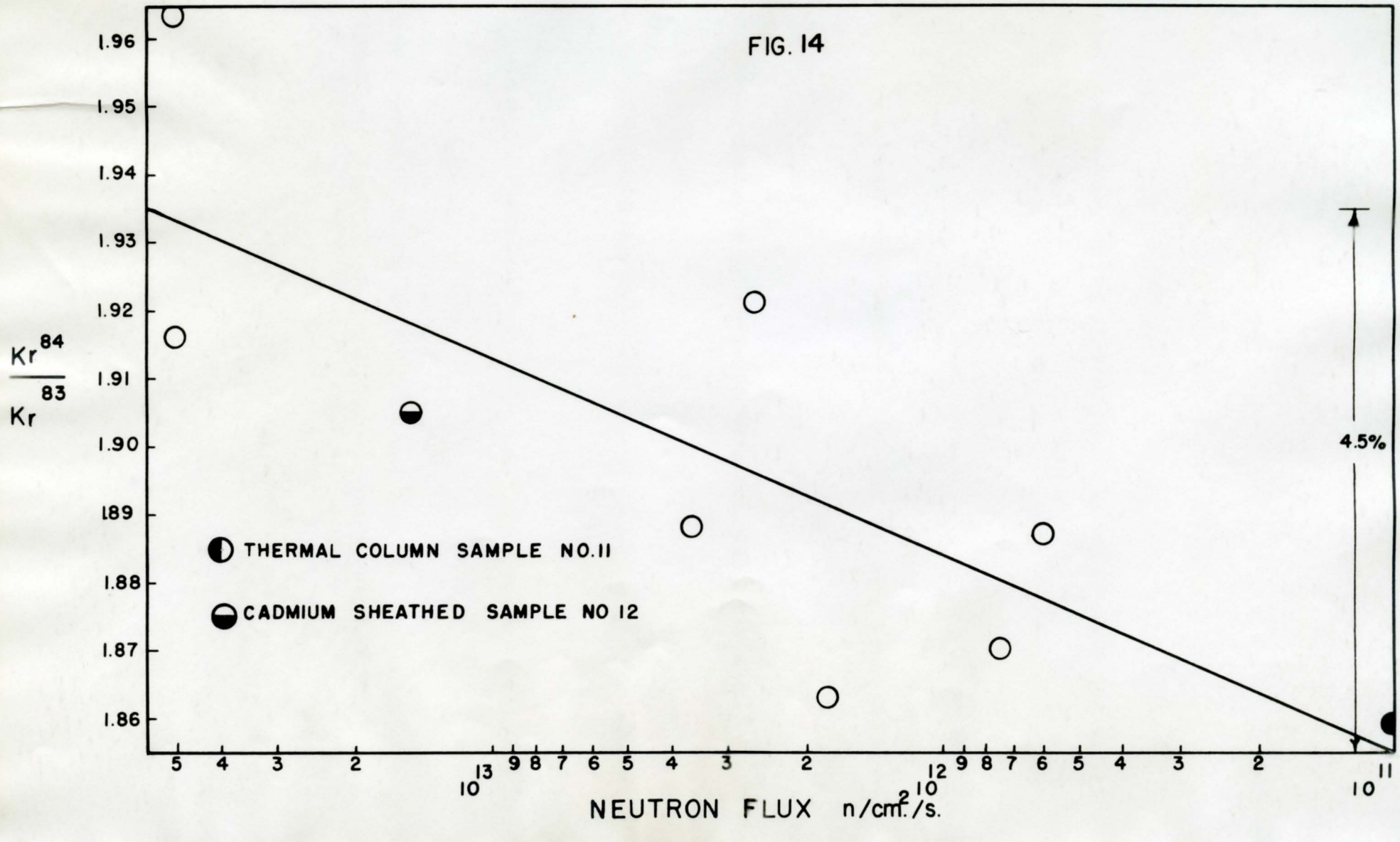
1.96
1.95
1.94
1.93
1.92
1.91
1.90
1.89
1.88
1.87
1.86
Kr 84 / Kr 83
4.5%
THERMAL COLUMN SAMPLE NO.11
CADMIUM SHEATHED SAMPLE NO 12
5 4 3 2 10^13 9 8 7 6 5 4 3 2 10^12 9 8 7 6 5 4 3 2 10^11
NEUTRON FLUX n/cm.²/s.

TABLE IX

FISSION PRODUCT KRYPTON ABUNDANCE DATA USED TO ESTABLISH CURVES OF FIGS. 15 AND 16.

Sample No.	Mass No.	Atom %	Fission Yield[a] %	Total Mass 85 Chain Yield[b] %	% Fission Yield			
					Sample 15 Reduced To 1.66% at Mass 86	Sample 15 Reduced To 0.80% at Mass 86	Sample 13 & 14 Adjusted For 60% U^{238} Fission	Sample 12 Adjusted For 20% U^{238} Fission
11	83	14.12	0.50					
	84	26.25	0.93					
	85	7.53	0.27	1.20				
	86	52.10	1.84					
12	83	14.05	0.50					0.45
	84	26.76	0.95					0.85
	85	7.69	0.274	1.22				1.09
	86	51.51	1.83					1.63
13 & 14	83	14.53	0.50				0.35	
	84	28.71	0.99				0.70	
	85	6.48	0.223	0.99			0.70	
	86	50.29	1.73				1.22	
15	83	14.52	0.50		0.49	0.24		
	84	30.80	1.06		1.035	0.50		
	85	5.23	0.18	0.80	0.78	0.38		
	86	49.46	1.70		1.66	0.80		

[a]Krypton isotope abundance data relative to a fission yield of 0.50% for mass 83.

[b]The mass 85 chain yield has been corrected for the decay of the 4.4 hr. isomer of Kr^{85} by placing the mass 85 yield on the smooth mass yield curve for sample No. 11 (U^{235} + n fission). This gives a branching ratio between the isomeric states of Kr^{85} of 0.27/(1.20-0.27) = 0.29. The mass 85 chain yields for the other samples have been ratioed up assuming that the branching ratio remains constant for U^{235} + n and U^{238} + n fission.

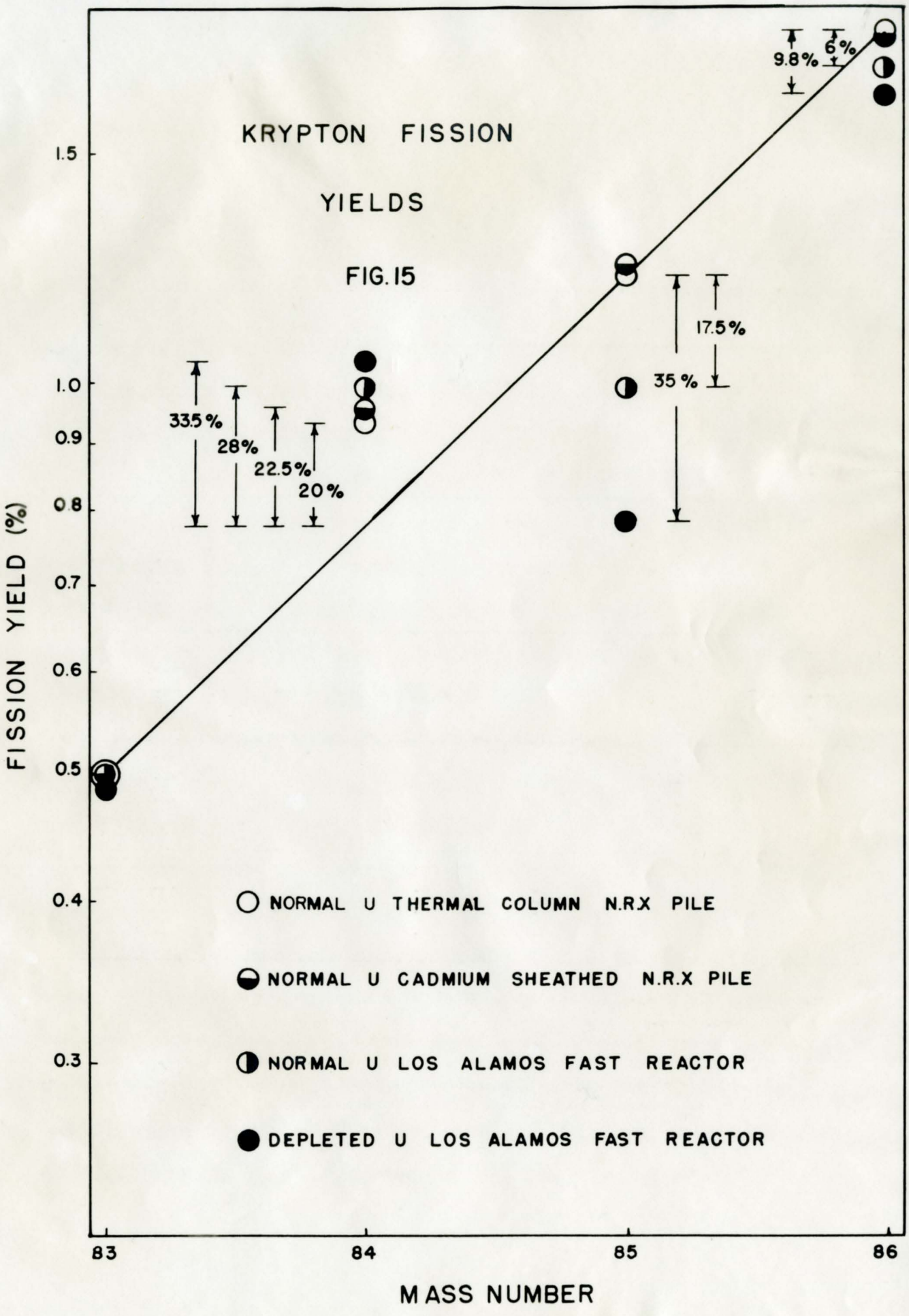
KRYPTON FISSION
YIELDS
FIG. 15
FISSION YIELD (%)
1.5
1.0
0.9
0.8
0.7
0.6
0.5
0.4
0.3
33.5%
28%
22.5%
20%
9.8%
6%
17.5%
35%
NORMAL U THERMAL COLUMN N.RX PILE
NORMAL U CADMIUM SHEATHED N.R.X PILE
NORMAL U LOS ALAMOS FAST REACTOR
DEPLETED U LOS ALAMOS FAST REACTOR
83
84
85
86
MASS NUMBER

fission yields in this mass range have not been firmly established. Since the Xe/Kr ratio, in which there is a discrepancy between reported values (8, 24), is required before the krypton and xenon yields may be related to one another, this ratio must be redetermined. However, the normalization factor used will not alter the conclusions drawn here. The depleted UO_3 yields have been adjusted, as in the xenon range, so that the Los Alamos normal uranium yields indicate the same percentage fine structure shift from the smooth curve for U^{235} + n fission, at masses 84 and 86. When this is done it is apparent that large yield variations occur at masses 84 and 86 and that approximately 60% U^{238} + n fission,(for example, 8 ÷ 13.5 = 59% at mass 84 and 6 ÷ 9.8 = 61% at mass 86) has taken place in the Los Alamos normal uranium sample, the same proportion that was determined for this sample from the xenon isotope fission yields.

The krypton isotope at mass 85 has two isomers, (Fig. 17) a long-lived one with a half-life of 10.27 yr. and a short-lived one with a 4.4 hr. half-life. Since the shorter-lived isomer will have completely decayed before the fission gases were extracted from the uranium discs, the mass spectrometer results will only indicate the yield of the 10.27 yr. isomer. All krypton yields have been corrected for the decay of the long-lived isomer up to the time of analysis. In order to compare the fission yields at this mass the Kr^{85} yield for the thermal column sample (U^{235} + n fission) has been placed on the smooth curve and the yields for the other samples have been increased proportionately (Table IX, column 5). This correction does not bring the other Kr^{85}

yields into line, indicating fine structure at this mass also.

Actually there is a decided shift of the light mass peak for U^{235} + n and U^{238} + n fission (Fig. II). Figure 16 is a replot of Fig. 15 in which the depleted UO_3 yields have been displaced at mass 86 (Table IX) by 0.86% of fission to correspond to the above-mentioned shift. The Los Alamos normal uranium results have also been adjusted at mass 86 in accordance with an indicated 60% U^{238} + n fission. Finally, the cadmium-sheathed sample (No. 12) results were incorporated in Fig. 16 by adjusting the mass 86 yield to correspond to 20% U^{238} + n fission as found in the xenon studies. It is now possible to draw four roughly parallel smooth curves from which the percentage variations may be calculated. Again defining fine structure as the percentage variation from the respective smooth curves, these results indicate large fine structure shifts at masses 84 and 85.

It will be noted that at mass 84 the fission yields are all higher than the corresponding smooth curve values while at mass 85 the opposite effect is found. The fine structure shift in going from U^{235} + n fission to U^{238} + n fission amounts to 40 - 20 = 20% at mass 84 and 29% at mass 85.

The fine structure determined for the Los Alamos normal uranium (No. 13 & 14) and the cadmium-sheathed sample (No. 12) fall in the intermediate range and indicate 12 ÷ 20 = 60% and 3 ÷ 20 = 15% U^{238} + n fission respectively when calculated from the mass 84 fission yield values. However, when calculated from the yield values at mass 85, the corresponding U^{238} + n contributions indicated are 52% and 0%. The U^{238} + n contribution indicated for the Los Alamos sample amounts to 60% and 52% when calculated from mass 84 and mass 85 fine

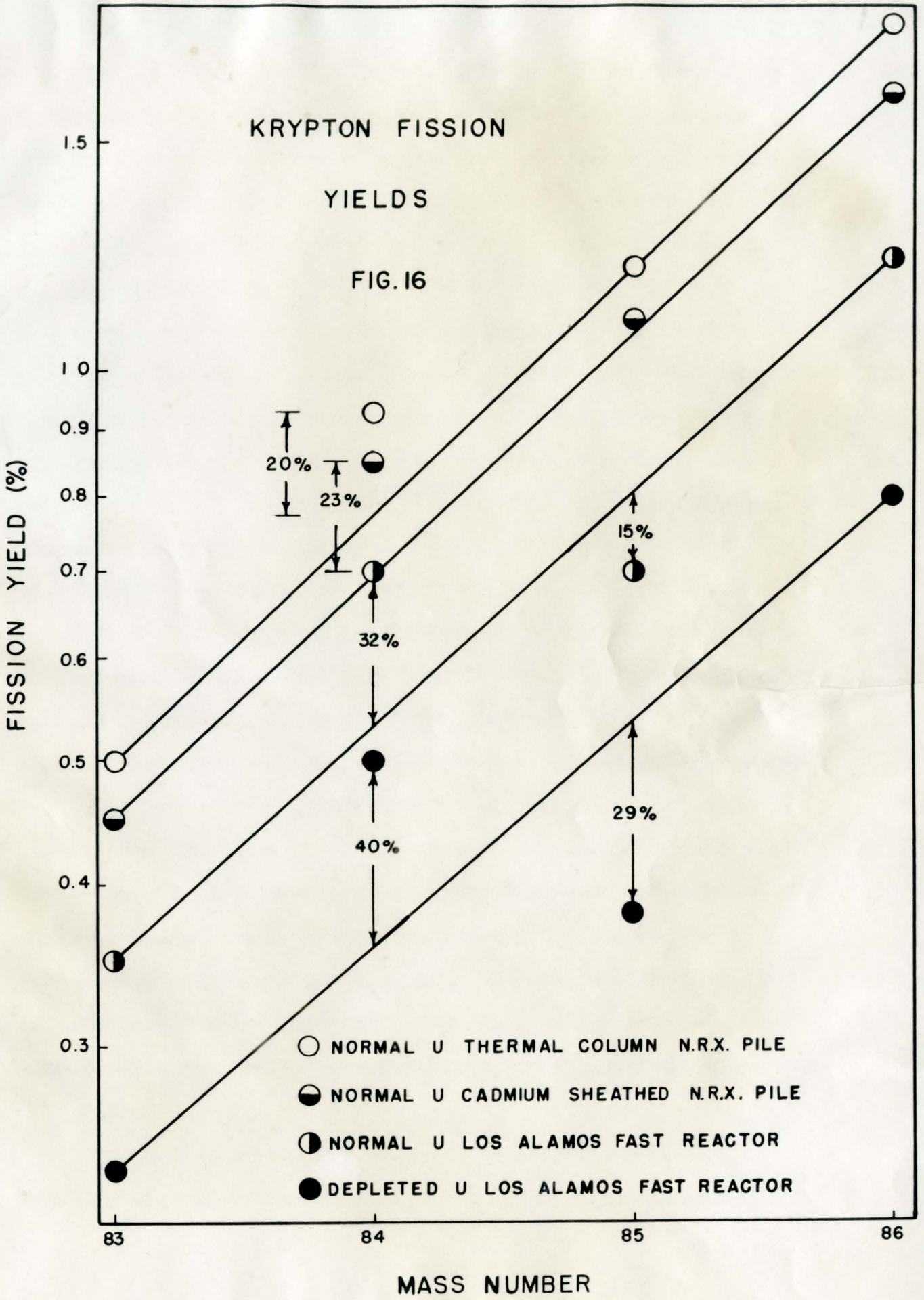
KRYPTON FISSION
YIELDS
FIG. 16
FISSION YIELD (%)
1.5
1.0
0.9
0.8
0.7
0.6
0.5
0.4
0.3
20%
23%
32%
40%
15%
29%
NORMAL U THERMAL COLUMN N.R.X. PILE
NORMAL U CADMIUM SHEATHED N.R.X. PILE
NORMAL U LOS ALAMOS FAST REACTOR
DEPLETED U LOS ALAMOS FAST REACTOR
83
84
85
86
MASS NUMBER

structure shifts respectively, in good agreement with the values found in the xenon range (57%). For the cadmium-sheathed sample the 15% U^{238} + n fission contribution indicated at mass 84 agrees with that found in the xenon range at mass 134 but does not agree at mass 85. This latter discrepancy may be due to the difficulty experienced in measuring the very small ion current recorded at mass 85 (see Fig. 5).

Since the mass 84 yields increase while those at mass 85 decrease, it may seem reasonable to account for this variation on the basis of neutron emission from mass 85 rather than the fine structure due to a structural preference for closed neutron shells in the initial fission act. However, Kr^{85} has 49 neutrons, one less than a closed shell, and the above reaction is considered to be highly improbable.

The existence of fine structure in the mass yield curve at masses 84 and 85 seems to be definitely established for the first time. The Glendenin mechanism (12) may be employed to predict the fine structure that may be expected as a result of the emission of the loosely bound 51st neutrons from the primary fission products. These calculations have been carried out and the predicted variations from the smooth curve values are given in Table X. A comparison of columns five and six shows that there is little agreement between predicted and observed fine structure in this mass range. It would seem, therefore, that the observed fine structure may be due to a preference for nuclides with 50 neutrons in the primary fission process or a combination of this and the Glendenin effect as was suggested by the results reported for xenon isotopes.

(c) Summary

Abnormal fission yields, resulting in fine structure in the mass fission yield curve, have been found in both the xenon and krypton

TABLE X

COMPARISON OF EXPERIMENTAL AND PREDICTED KRYPTON FISSION YIELDS

Fissioning nuclide	Mass Chain	Smooth curve yields[a] %	M.S. yields %	Departure from smooth curve %	Departure predicted by Glendenin mechanism %
U^{235}	83	0.50	0.50	-	+ 46
	84	0.77	0.93	+20	+ 18
	85	1.20	1.20[b]	-	- 8
	86	1.84	1.84	-	- 9
U^{238}	83	0.24	0.24	-	+ 25
	84	0.36	0.50	+ 40	-
	85	0.54	0.38[b]	- 29	- 13
	86	0.80	0.80	-	- 11

a See Fig. 16.

b Krypton yields at mass 85 have been corrected for decay of 4.4 hr. isomer.

mass ranges. A shift of the fine structure, to lower masses, has been observed when going from U^{235} + n fission to U^{238} + n fission. From the shift in fine structure it has been possible to determine the proportions of U^{235} and U^{238} neutron fission that have taken place in uranium samples under given irradiation conditions.

These abnormal yields are most probably due to the presence of closed neutron shells of 82 and 50 neutrons which fall in the xenon and krypton mass ranges respectively. There is evidence that this fine structure is to some extent due to a structural preference for these closed neutron shells in the initial fission act. The Glendenin mechanism, which involves the emission of the loosely held 83rd and 51st neutrons from the primary fission products, was postulated to account for this fine structure but does not in itself completely explain the experimentally observed fission yields. It may be that these effects are due to a combination of the two processes. Any comprehensive theory of the fission process must take into account the observed abnormal fission yields and the shifting of the fine structure for the fission of different uranium nuclei.

(iii) The Branching Ratio of Kr^{85m}

A branching ratio of 0.28 for the decay of the isomeric state of Kr^{85} has been reported by Bergström (28), who measured the ratio of internal conversion electrons to β^- rays and corrected for the conversion probability due to an M4 isomeric transition. The precise determination of the krypton fission product yields by mass spectrometric methods allows one to check the value obtained from the β spectrum analysis.

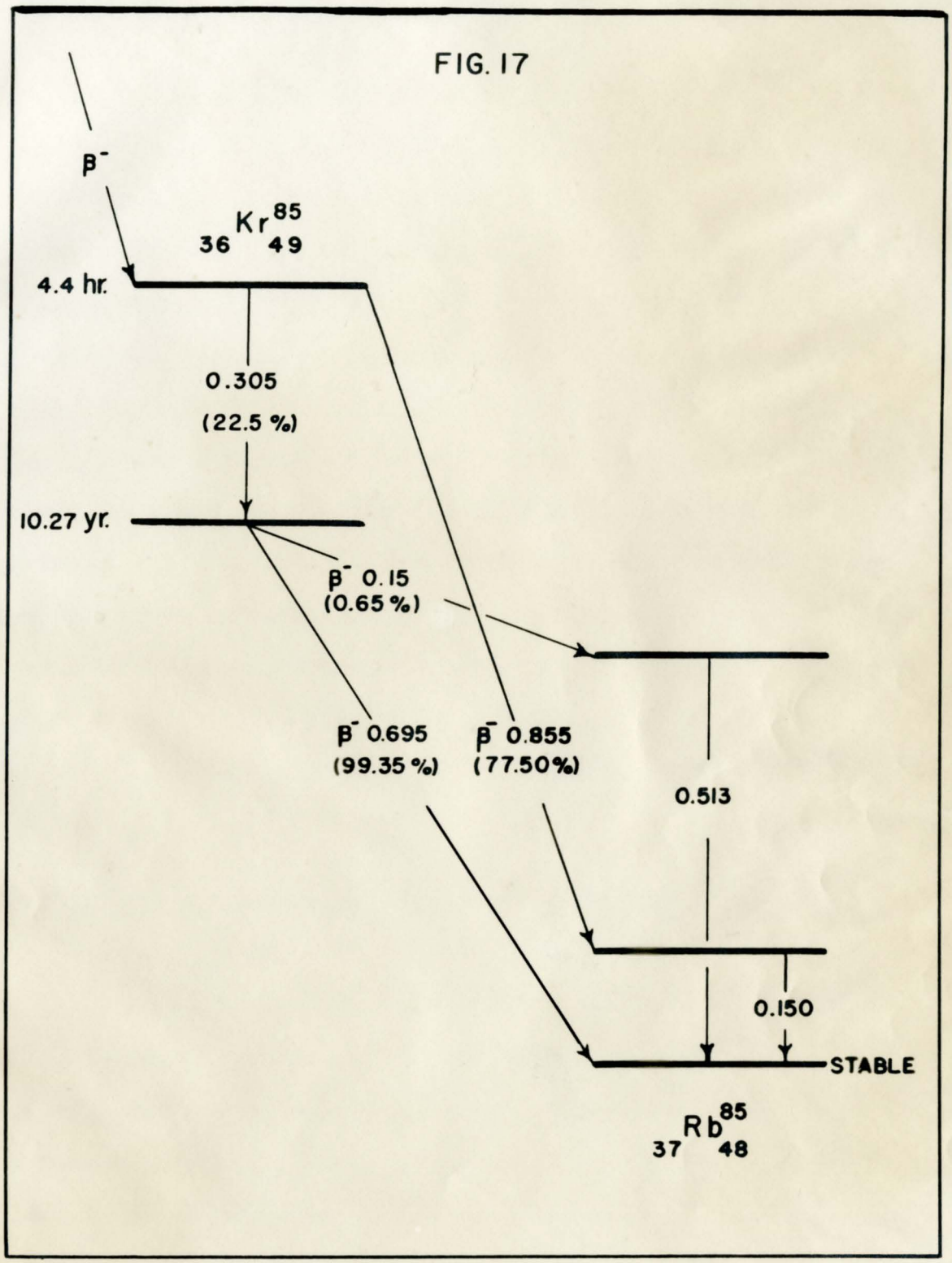

Kr^{85} DECAY SCHEME

The ion current (Fig. V) measured at mass 85 is due only to the 10.27 yr. isomer since the fission gases were extracted from the irradiated material after a long "cooling" period. The fission yield of the 10.27 yr. isomer was obtained by correcting the mass spectrometer abundance data for radioactive decay. In order to establish the krypton yield curves of Fig. 16 the yield of the 85 mass chain was placed on the smooth curve for U^{235} + n fission (thermal column sample No. 11). The percentage of the 85 mass chain decaying through the long-lived isomer was found to be 0.27 ÷ 1.20 or 22.5%, which yields a branching ratio of 0.29. This is in excellent agreement with the value reported by Bergström and supports the conclusion that the Kr^{85} mass yield falls on the smooth fission yield curve indicating no fine structure at this mass for U^{235} + n fission.

Figure 17 illustrates the complete decay scheme for Kr^{85} (28) (27).

(iv) The Mass Spectrometer Determination of the Half-life of Kr^{85}

Prior to 1945 the only Kr^{85} isomer known had a 4.5 hr. half-life, an activity first noted by Snell (29) in 1937 while studying the (d, p) reaction on Kr. In 1945 Hoagland and Sugarman (30) found an activity with a minimum half-life of 10 years when investigating the gaseous activities in fission products. They were able to show that this was due to an isotope of krypton and assigned it either to Kr^{85} or Kr^{87}. Thode and Graham (8) of the Canadian Atomic Energy Project independently discovered a long-lived isotope of krypton during investigation of gaseous fission products with a mass spectrometer. Their results showed the definite existence of a long-lived isotope of krypton

at mass 85 and hence an isomer of the known 4.5 hr. krypton of that mass. The mass spectrometer work also indicated that the fission yield of this isomer was about 25% of the total yield of the 85 mass chain. By following the decrease of this isotope over a period of a few months Thode and Graham were able to show that it decayed with a half-life of about 9.4 years. With this additional information the uncertainty in the mass assignment of the activity reported by Hoagland and Sugarman was removed and the 10 year activity was attributed to Kr^{85}.

The early mass spectrometer determinations were not too precise since measurements were made on samples that had only decayed a short time. However, with these samples almost seven years old it has been possible to redetermine the half-life of Kr^{85} with improved accuracy. The results obtained are reported below.

Half-life measurements by the mass spectrometer method involve the determination of the concentration of the radioactive isotope relative to a stable isotope after various time intervals. These measurements are most accurate when the elapsed time between two isotope ratio determinations is of the order of the half-life of the isotope being investigated, which in the case of Kr^{85} is approximately ten years. In the work reported here the Kr^{85} concentration was determined relative to both the stable isotope Kr^{84} and the stable isotope Kr^{86}, thus eliminating any mass discrimination that may be inherent in the mass spectrometer. The equation $N = N_o e^{-\lambda t}$, where N is the concentration at time t, N_o the concentration at zero time, and λ the disintegration constant, was used in the determination. By substituting the mass spectrometer ratios

Kr^{85}/Kr^{84} and Kr^{85}/Kr^{86}, obtained after different time intervals, for N/N_o, the half-life may be calculated from the relation $T_{\frac{1}{2}} = 0.6931/\lambda$. The ratios Kr^{85}/Kr^{84} and Kr^{85}/Kr^{86} obtained in 1946 were substituted for N_o in all the calculations.

A few uranium discs irradiated in 1945 were available in this laboratory. Two of these were dissolved and the fission gases extracted using the techniques developed by Arrol, Chackett, and Epstein (24). Since there are indications that small variations in fission yields occur depending on irradiation conditions, it was felt that a more reliable result could be obtained if the same gas studied in 1946 was re-analyzed. A sample of the original gas was, therefore, purified in a calcium furnace (Fig. 4) and the small amount (< 0.001 cc.) of gas remaining was analyzed in both the krypton and xenon mass ranges. The results of this determination are included in Table XII as run No. 7.

Table XI gives the relative mass spectrometer abundance data for the krypton isotopes obtained for sample L in 1946 and 1952. The decrease in the Kr^{85} abundance over a period of nearly seven years is readily apparent.

The half-life results obtained from seven different mass spectrometer runs made on samples F, K, and L are given in Table XII. Uranium samples F and K were irradiated at the same time (1945)and in adjacent positions to sample L, which was investigated first in 1946. It is, therefore, reasonable to assume similar irradiation conditions for the three uranium samples. The results of run 7, given in Table XII, are, of course, not dependent on this assumption. The Kr^{85} half-life determined from the average of these results was found to be

TABLE XI

ABUNDANCE DATA FOR ISOTOPES OF FISSION PRODUCT KRYPTON SAMPLE L

DETERMINED WITH A 180 DEGREE MASS SPECTROMETER

Mass Unit	1946 Atom %	1952 Atom %
83	14.25 ± 0.04	14.55 ± 0.01
84	26.76 ± 0.01	27.50 ± 0.01
85	7.43 ± 0.01	4.85 ± 0.01
86	51.52 ± 0.04	53.09 ± 0.02

TABLE XII

Kr^{85} HALF-LIFE FROM MASS SPECTROMETER ABUNDANCE DATA

Run No.	Sample No.	Elapsed Time (in days)	Kr^{85} $T_{\frac{1}{2}}$ (in years) Calculated From		Average
			Kr^{85}/Kr^{84}	Kr^{85}/Kr^{86}	
1	F	2027	9.95	10.11	10.03
2	K	2167	10.53	10.38	10.46
3	K	2168	10.64	10.39	10.52
4	K	2176	10.44	10.42	10.43
5	K	2176	10.34	10.09	10.22
6	K	2176	10.20	9.98	10.09
7	L	2439	10.19	10.13	10.16
					10.27 ± 0.18* yrs.

*Standard Deviation

10.27 ± 0.18 years.

As mentioned above the purified gas from disc L was analyzed in both the krypton and xenon mass ranges. Tables XIII and XIV compare the stable krypton and xenon isotope abundances determined in 1946 and 1952. The percentage differences shown indicate agreement within 1% which is indeed remarkable in view of the fact that the mass spectrometer has been completely rebuilt in the interval. We can, therefore, have considerable confidence in the isotope ratios obtained in 1946 which are used together with the more recent values to determine the half-life of Kr^{85}. The mass spectrometer is now equipped with a vibrating reed electrometer and automatic recording, hence more precise determinations are possible.

TABLE XIII

COMPARISON OF ABUNDANCE DATA FOR STABLE ISOTOPES OF FISSION PRODUCT KRYPTON SAMPLE L DETERMINED WITH A 180 DEGREE MASS SPECTROMETER

Mass Unit	1946 Atom %	1952 Atom%	% Difference
83	15.40 ± 0.04	15.29 ± 0.01	-0.71
84	28.92 ± 0.01	28.90 ± 0.01	-0.07
86	55.68 ± 0.04	55.80 ± 0.02	+0.20

TABLE XIV

COMPARISON OF ABUNDANCE DATA FOR ISOTOPES OF FISSION PRODUCT XENON SAMPLE L DETERMINED WITH A 180 DEGREE MASS SPECTROMETER

Mass Unit	1946 Atom %	1952 Atom %	% Difference
131	13.38 ± 0.04	13.39 ± 0.01	+0.07
132	20.09 ± 0.04	20.01 ± 0.01	-0.40
134	35.76 ± 0.04	36.00 ± 0.02	+0.67
136	30.77 ± 0.04	30.63 ± 0.02	-0.45

BIBLIOGRAPHY

1. Segre E., Phys. Rev. 86, 21, (1952).

2. Ghiorso A., Higgins G. H., Larsh A. E., Seaborg G. T., Thompson S. G., Phys. Rev. 87, 163, (1952).

3. Hahn O., Strassmann F., Naturwiss., 27, 11, (1939).

4. Ogle W. E., McElhinney J., Phys. Rev. 81, 344, (1951).

5. Nuclear Constants for Reactor Studies, Can. J. of Physics, 30, 624, (1952).

6. Steinberg E. P., Freedman M. S., National Nuclear Energy Series. Division IV. Volume 9. Part V. McGraw-Hill Book Company Inc., New York, Toronto and London. 1951. p. 1378.

7. Way K., Wigner E. P., Phys. Rev. 73, 1318, (1948).

8. Thode, H. G., Graham R. L., Report MX-129, National Research Council April 1945; Can. J. Research, A, 25, 1, (1947).

9. Wiles D. R., Smith B. W., Horsley R., Thode H. G., Can. J. Physics, 31, 419, (1953).

10. Graham R. L., Harkness A. L., Thode H. G., J. Sci. Instruments, 24, 119, (1947).

11. Macnamara J., Collins C. B., Thode H. G., Phys. Rev. 78, 129, (1950).

12. Glendenin L. E., Ph.D. Thesis, Massachusetts Institute of Technology, July, 1949.

13. Mayer M. G., Phys. Rev. 74, 235, (1948).

14. Harvey J. A., Phys. Rev., 81, 353, (1951).

15. Wiles, D. R., M.Sc. Thesis, McMaster University. 1950.

16. Glendenin L. E., Steinberg E. P., Inghram M. G., Hess D. C., Phys. Rev. 84, 860, (1951).

17. Duckworth H. E., Preston R. S., Phys. Rev. 82, 468, (1951).

18. Spence R. W., Atomic Energy Commission Unclassified Document BNL-C-9, 1949 (unpublished), Brookhaven Chemistry Conference No. 3.

19. Turkevich A., Niday J. B., Phys. Rev. 84, 52, (1951).

20. Turkevich A., Niday J. B., Tompkins A., Phys. Rev. 89, 552, (1953).

21. Schmitt R. A., Sugarman N., Phys. Rev. 89, 1155, (1953).

22. Meitner L., Nature 165, 561, (1950).

23. Bohr N., Wheeler J. A., Phys. Rev. 56, 426, (1939).

24. Arrol W. J., Chackett K. F., Epstein S., Can. J. Research B, 27, 757, (1949).

25. Neutron Cross Sections, AECU-2040, May 15, 1952.

26. Wilson I. L., Some Data on Pile Irradiations, Chalk River Report No. CRE-414, March, 1949.

27. Bergström I., M. Siegbahn Commemorative Volume, XX, Uppsala, 1951, p. 355.

28. Goldhaber M., Hill R. D., Rev. Mod. Phys. 24, 179, (1952).

29. Snell A. H., Phys. Rev. 52, 1007, (1937).

30. Hoagland E. J., Sugarman N., National Nuclear Energy Series, Division IV. Volume 9. Part V. McGraw-Hill Book Company Inc., New York, Toronto and London. 1951, p. 635.